



Volatility-dependent probability weighting and the dynamics of the pricing kernel puzzle

Maik Dierkes¹ · Jan Krupski¹ · Sebastian Schroen¹ · Philipp Sibbertsen²

Accepted: 16 October 2023 / Published online: 29 November 2023
© The Author(s) 2023

Abstract

In order to estimate volatility-dependent probability weighting functions, we obtain risk neutral and physical densities from the Pan (J Financ Econ 63(1):3–50, 2002. [https://doi.org/10.1016/S0304-405X\(01\)00088-5](https://doi.org/10.1016/S0304-405X(01)00088-5)) stochastic volatility and jumps model. Across volatility levels, we find pronounced inverse S-shapes, i.e. small probabilities are overweighted, and probability weighting almost monotonically increases in volatility, indicating higher skewness preferences and crash aversion in volatile market environments. Moreover, by estimating probabilistic risk attitudes, equivalent to the share of risk aversion related to probability weighting, we shed further light on the pricing kernel puzzle. While pricing kernels estimated from the Pan (J Financ Econ 63(1):3–50, 2002. [https://doi.org/10.1016/S0304-405X\(01\)00088-5](https://doi.org/10.1016/S0304-405X(01)00088-5)) model display the typical U-shape as documented in the literature, pricing kernels—net of probability weighting—are strictly monotonically decreasing and thus in line with economic theory. Equivalently, we find risk aversion to be positive across wealth levels. Our results are robust to alternative maturities, wealth percentiles, alternative functional forms, a nonparametric empirical setting and variations of the Pan (J Financ Econ 63(1):3–50, 2002. [https://doi.org/10.1016/S0304-405X\(01\)00088-5](https://doi.org/10.1016/S0304-405X(01)00088-5)) coefficient estimates.

Keywords Volatility · Probability weighting · Pricing kernel puzzle · Risk preferences

JEL Classification G11 · G14 · G41

1 Introduction

According to Jackwerth (2000), risk neutral probabilities are tantamount to the product of physical probabilities and a risk aversion adjustment. The pricing kernel, defined as the ratio of risk neutral and physical probabilities, is expected to monotonically decrease in wealth and distinctly reflects risk aversion. However, several

Extended author information available on the last page of the article

studies find U-shaped pricing kernels (the pricing kernel puzzle) or, equivalently, negative episodes of risk aversion functions (the risk aversion puzzle). We attribute this finding to investors who overweight small probabilities for tail events and therefore distort the pricing kernel. Moreover, it has long been suggested that time-varying risk aversion or, put differently, a time-varying price of risk, is key to understand asset prices. For example, Fama (2014) notes that both risk and investors' risk aversion are likely to change over time, resulting in a time-varying equity premium. In line with this, we refer time variation in pricing kernels and risk aversion to a volatility-dependent and hence time-varying degree of probability weighting.

Our study thus contributes to two strands of literature: *time-varying risk preferences* and the *pricing kernel puzzle*. First, we obtain risk neutral and physical densities from the Pan (2002) stochastic volatility and jumps model and find a strikingly robust relationship between volatility and Cumulative Prospect Theory (CPT)'s probability weighting parameter γ (see Tversky and Kahneman, 1992). Across volatility levels, the probability weighting function exhibits an inverse S-shape, i.e. small (large) probabilities are overweighted (underweighted) and γ (probability weighting) almost monotonically decreases (increases) in volatility, suggesting that skewness preferences and crash aversion are more pronounced in volatile markets. Second, consistent with our hypothesis, it is the probabilistic risk attitude that produces the puzzling U-shape of the pricing kernel. In other words, pricing kernels net of probability weighting are strictly monotonically decreasing and therefore in line with economic theory. As a direct result, risk aversion functions net of probability weighting are positive throughout wealth levels.

In a seminal study, Campbell and Cochrane (1999) propose a habit-formation model with slowly moving external habits and find both risk aversion and marginal utility to countercyclically depend on the business cycle. Moreover, the model explains several asset pricing phenomena, including the procyclical (countercyclical) variation of stock prices (volatility). Brandt and Wang (2003) extend the habit-formation model by including a process for aggregate risk aversion and also find risk preferences to vary. They conclude their results to be consistent with both, an agent irrationally fearing unexpected inflation, and an economy with heterogeneous preferences where risk aversion varies with the cross-sectional distribution of wealth. In a more recent study, Guiso et al. (2018) analyze portfolio data and repeated surveys of Italian bank clients in 2007 and 2009. After the financial crisis, they find both qualitative and quantitative measures of risk aversion to increase substantially. As potential mechanisms behind their findings, the authors suggest fear of losses and overweighting of salient payoffs. Hence, it seems reasonable to explain time-varying risk preferences from a behavioral perspective. In this sense, Barberis et al. (2001) propose a prospect theory framework in which, in contrast to Campbell and Cochrane (1999), changes in risk aversion are caused by changes in the level of the stock market. They find that, after recent run-ups, agents are less risk averse because prior gains cushion subsequent losses. In comparison to consumption-based models, the level of risk aversion is smaller but still explains several market characteristics. While Barberis et al. (2001) restrict their model to reference-point dependent valuation and loss aversion, several recent studies highlight the importance of CPT's probability weighting component. Kliger and Levy (2009) assess the performance of

expected utility (EUT), rank-dependent expected utility (RDEU), and CPT models and find that probability weighting functions exhibit a pronounced inverse S-shape.¹ Moreover, when including probability weighting, the model fit improves substantially. Polkovnichenko and Zhao (2013) and Dierkes et al. (2022) estimate option-implied probability weighting functions and find them to substantially vary over time. Notably, variation is not erratic, but systematic. For example, Kilka and Weber (2001) find in the lab that probability weighting is more pronounced when agents are less confident in assessing the uncertainty of a decision situation – much like in a high volatility regime, especially when volatility drives up jump intensity. In line with this finding, Liu et al. (2005) propose that risk and rare events should have an impact on risk preferences and Chabi-Yo et al. (2008) relate changes in preferences and beliefs to regime shifts in state variables.² Moreover, Gao et al. (2021) show that investors dislike high-skewness securities in low volatility regimes, while Polkovnichenko and Zhao (2013) note that periods with less inverse S-shaped probability weighting functions tend to coincide with these regimes.

We capture these findings by estimating volatility-dependent probability weighting functions from the Pan (2002) stochastic volatility and jumps model. We choose simulations within this model as it offers the advantage that, in addition to the wealth level, it includes the volatility as an additional state variable which we can change counterfactually (with all else being equal). Compare this to an empirical setting where changes in volatility can only be observed over time and it is impossible to rule out unobserved factors other than volatility as drivers of probability weighting. Furthermore, note that probability weighting is particularly sensitive to estimates of the tails of physical and risk neutral distributions. The structural approach of the Pan (2002) model, calibrated to the options market and S&P 500 returns, avoids the noise of nonparametric tail estimates. Nevertheless, in a robustness check, we also refer to nonparametric estimates of physical and risk neutral probabilities and find our model-based results to hold in a fully nonparametric setting.

Following Ziegler (2007), we first obtain risk neutral and physical densities for a wide range of volatilities. Thereafter, we follow Dierkes et al. (2022) and employ these densities to estimate the probability weighting parameter γ for any given volatility. Even though the Pan (2002) model was never designed to match CPT preferences, our results are strikingly robust and correspond to earlier studies. In our main specification, we normalize the return horizon to one year and find γ (probability weighting) to almost monotonically decrease (increase) in volatility. For example, with the two-parameter specification of Prelec (1998), γ s vary from roughly 0.99 for very low volatilities to 0.70 for high volatilities. Results for the two-parameter linear-in-log-odds (0.90–0.68) and the one-parameter Tversky and Kahneman (1992) function (0.95–0.82) are similar. Most importantly, we find the average probability weighting function over volatilities to display a pronounced inverse

¹ See also Camerer and Ho (1994), Tversky and Fox (1995), Wu and Gonzalez (1996), Gonzalez and Wu (1999), Abdellaoui (2000), and Bleichrodt and Pinto (2000).

² See also Bliss and Panigirtzoglou (2004) and Brown & Jackwerth (2012).

S-shape. These findings are robust to alternative return horizons (three months and six months) and a nonparametric empirical setting.

As risk aversion is closely connected to the pricing kernel, we can directly transfer our estimation approach to the pricing kernel puzzle. In a seminal study, Jackwerth (2000) recovers risk aversion from risk neutral and physical probabilities, estimated via S&P 500 options and stock returns, respectively.³ While he finds risk aversion to be positive and decreasing in wealth prior to the 1987 stock market crash, risk aversion is partially negative and increasing in the post-crash era. Among others, the puzzle has been confirmed by Ait-Sahalia and Lo (2000) and Rosenberg and Engle (2002). Moreover, Beare and Schmidt (2016) and Golubev et al. (2014) perform statistical tests and reject pricing kernel monotonicity for the S&P 500 and the German DAX, respectively.⁴ In the recent past, several studies proposed possible solutions to the pricing kernel puzzle. For example, Bakshi et al. (2010) assume heterogeneity among investors, with pessimists short selling the market portfolio and thus driving increases in the pricing kernel. Ziegler (2007) estimates risk aversion functions from the Pan (2002) model and finds them to be monotonically decreasing but negative for gains (implying an increasing pricing kernel). Although assuming heterogeneous investors might solve the problem, the degree of heterogeneity would need to be implausibly large. Further possible solutions include state-dependence in fundamentals (Chabi-Yo et al., 2008) and the inclusion of higher moment preferences (Chabi-Yo, 2012; Cuesdeanu and Jackwerth, 2018). Hens and Reichlin (2013) show that if at least one of the three standard assumptions (market completeness, risk aversion, correct beliefs) is violated, the pricing kernel may have increasing parts. Most importantly, they find the combination of distorted beliefs (i.e. probability weighting) and misestimation of probabilities to be a possible solution.⁵ Hence, it appears reasonable that applying behavioral insights may solve the pricing kernel puzzle.

In this sense, Baele et al. (2019) develop an asset pricing model with CPT preferences (based on Barberis et al., 2001) and find the implied CPT pricing kernel to display a pronounced U-shape (implying partially negative risk aversion functions). In line with Barberis et al. (2016), they conclude that the key driver of their results is the probability weighting component. Polkovnichenko and Zhao (2013) and Dierkes et al. (2022) estimate pricing kernels to study the time variation in probability weighting functions. While their results are generally consistent with a U-shaped pricing kernel, they rather focus on the time variation in probability weighting and its asset pricing implications.

³ To obtain densities, Jackwerth (2000) employs a variation of Jackwerth and Rubinstein (1996)'s approach.

⁴ Bliss and Panigirtzoglou (2004) find risk aversion estimates to be positive. However, they restrict the pricing kernel by assuming power or exponential utility functions. Linn et al. (2018) argue that prior pricing kernel estimates are inconsistent because they compare forward looking risk neutral densities to backward looking physical densities. While they find a monotonically decreasing pricing kernel, Cuesdeanu and Jackwerth (2018) attribute this result to their specific estimation procedure.

⁵ However, they need to assume a slightly negative expected mean return.

By adjusting model-implied pricing kernels and risk aversion functions for probability weighting, we shed further light on the role of probability weighting as an important driver of the pricing kernel puzzle. Since Benzoni et al. (2011) and Babaoğlu et al. (2018) find pricing kernels to be variance-dependent, we again employ the Pan (2002) stochastic volatility and jumps model and estimate probabilistic risk attitudes, equivalent to the share of risk aversion related to probability weighting.⁶ We add to the results of previous studies in two ways. First, we provide direct measures of pricing kernels and risk aversion functions, and second, we explicitly relate the pricing kernel puzzle to the probabilistic risk attitude. Before accounting for probability weighting, we find the average pricing kernel to exhibit a strong U-shape, implying episodes of negative risk aversion (consistent with Ziegler, 2007). However, since the probabilistic risk attitude is strikingly close to the risk aversion estimated from Pan (2002), the adjusted risk aversion function is consistently positive and the corresponding pricing kernel is monotonically decreasing in wealth. Our results are robust to alternative return horizons (3 and 6 months), wealth percentiles, an alternative functional assumption, a numerical approach to estimate the probabilistic risk attitude, and variations of the Pan (2002) coefficient estimates. We therefore conclude that probability weighting intensifies in volatile market environments and plays an important role in explaining the pricing kernel puzzle.

2 Methodology

2.1 Estimation of probability weights

Our framework closely follows Dierkes et al. (2022) who introduce a fully nonparametric estimation procedure to derive time-varying probability weighting functions. For the sake of brevity, we therefore limit this section to the most important components and refer to their study for more details.

By assuming a representative agent who derives utility from the market return S and has both a monotonically increasing and twice continuously differentiable utility function u and probability weighting function w , we yield the pricing kernel, net of probability weighting, as

$$\frac{f_Q(S_T)}{f_P(S_T) \cdot w'(1 - F_P(S_T))} = \beta \frac{u'(S_T)}{u'(S_t)}, \quad (1)$$

where $f_Q(S_T)$ and $f_P(S_T)$ denote the risk neutral and physical densities with corresponding distribution functions F_Q and F_P . Moreover, $u'(S_T)$ and $u'(S_t)$ are marginal utilities with respect to the future and current stock price, respectively, and β is a normalizing constant. Note that the adjusted pricing kernel varies with the physical distribution, $F_P(S_T)$, if w is not linear. In case of linear w , however, Eq. (1) collapses

⁶ Further studies that relate the pricing kernel and risk aversion to volatility are Christoffersen et al. (2013), Song and Xiu (2016), and Linn et al. (2018).

to the standard pricing kernel, i.e. the ratio of risk neutral to physical probabilities. Taking the logarithm on both sides of Eq. (1) then gives

$$\log \left(\frac{f_Q(S_T)}{f_P(S_T) \cdot w'(1 - F_P(S_T))} \right) = \log \left(\beta \frac{u'(S_T)}{u'(S_t)} \right), \quad (2)$$

which is equivalent to

$$\log(f_Q(S_T)) - \log(f_P(S_T)) - \log(w'(1 - F_P(S_T))) = \log \left(\frac{\beta}{u'(S_t)} \right) + \log(u'(S_T)). \quad (3)$$

Adding the term with the probability weighting function on both sides and multiplying by -1 then yields

$$\log(f_P(S_T)) - \log(f_Q(S_T)) = -\log \left(\frac{\beta}{u'(S_t)} \right) - \log(u'(S_T)) - \log(w'(1 - F_P(S_T))). \quad (4)$$

Next, we take the derivative with respect to S_T . Noting that the first term on the right hand side is a constant, we obtain the absolute risk aversion function, $ARA(S_T)$, with probability weighting

$$\underbrace{\frac{f'_P(S_T)}{f_P(S_T)} - \frac{f'_Q(S_T)}{f_Q(S_T)}}_{ARA(S_T)} = \underbrace{-\frac{u''(S_T)}{u'(S_T)}}_{ARA_u(S_T)} + \underbrace{\frac{w''(1 - F_P(S_T))}{w'(1 - F_P(S_T))} f_P(S_T)}_{ARA_w(S_T)}, \quad (5)$$

where $ARA_u(S_T)$ denotes the absolute risk aversion after accounting for probability weighting, i.e. the level of risk aversion only associated with the utility function u . In contrast, $ARA_w(S_T)$ describes the *probabilistic risk attitude* and reflects the level of risk aversion originating from the probability weighting function w .⁷ Moreover, Eq. (5) reveals that without probability weighting, the probabilistic risk attitude becomes zero and absolute risk aversion boils down to Jackwerth (2000)'s Eq. (4). An expression of relative risk aversion is easily derived by multiplying both sides of Eq. (5) with S_T (see e.g. Eq. (5.3) in Ait-Sahalia and Lo, 2000):

$$\underbrace{S_T \frac{f'_P(S_T)}{f_P(S_T)} - S_T \frac{f'_Q(S_T)}{f_Q(S_T)}}_{RRA(S_T)} = \underbrace{-S_T \frac{u''(S_T)}{u'(S_T)}}_{RRA_u(S_T)} + \underbrace{S_T \frac{w''(1 - F_P(S_T))}{w'(1 - F_P(S_T))} f_P(S_T)}_{RRA_w(S_T)}, \quad (6)$$

where RRA_u and RRA_w denote the relative risk aversion associated with u and w , respectively. In case of the typically observed inverse S-shaped probability weighting function, the probabilistic risk attitude is positive (and decreasing) for low

⁷ By assuming an increasing probability weighting function, the denominator of the probabilistic risk attitude is always positive. See also Polkovnichenko and Zhao (2013) and Quiggin (1993).

wealth levels and negative for high wealth levels. Thus, convex episodes of the probability weighting function increase the observed risk aversion ($ARA_w(S_T) > 0$ or equivalently $RRA_w(S_T) > 0$), while concave parts reduce it ($ARA_w(S_T) < 0$ or equivalently $RRA_w(S_T) < 0$). For example, consider the probability weighting function $w(p) = p^\gamma$. Although it does not feature the typically observed inverse-S shape, it serves as an easy to understand example since it holds $w''(p)/w'(p) = \frac{\gamma-1}{p}$, so that

$$RRA_w(S_T) = S_T \cdot f_P(S_T) \frac{\gamma - 1}{1 - F_P(S_T)}.$$

For $\gamma \in (0, 1)$, this probability weighting function is strictly concave for all $p \in [0, 1]$ and RRA_w is negative for all wealth levels. Thus, relative risk aversion RRA is reduced by RRA_w . Intuitively, this probability weighting function transfers probability mass to higher wealth states and, thus, renders the representative investor more optimistic or risk prone relative to risk aversion RRA_u (associated only with the investor's utility function). If $\gamma > 1$, however, then w is convex and RRA_w is positive for all wealth levels and risk aversion increases because the investor behaves as if there is more probability mass moved to bad wealth states. As for the utility function, the constant relative risk aversion utility function $u(S_T)$, for example, implies that $RRA_u(S_T)$ is a constant c and $ARA_u(S_T) = \frac{c}{S_T}$.

To identify u and w , we do not assume any parametric form of u and w . Instead, we utilize the fact that probabilistic risk attitude, expressed by $RRA_w(S_T)$ or $ARA_w(S_T)$, varies with the physical distribution, $F_P(S_T)$, while $ARA_u(S_T)$ remains constant. Assuming two different physical distributions, $F_{P_1}(S_T)$ and $F_{P_2}(S_T)$, merging β and $u'(S_i)$ to a single normalizing constant β , and dropping the time index T for notional convenience then yields

$$w'(1 - F_{P_2}(S)) = \frac{f_{Q_2}(S) f_{P_1}(S) \beta_1}{f_{Q_1}(S) f_{P_2}(S) \beta_2} \cdot w'(1 - F_{P_1}(S)), \quad \forall S. \quad (7)$$

Since we are able to estimate risk neutral and physical densities from the Pan (2002) stochastic volatility and jumps model (see Sect. 2.2), Eq. (7) leaves w' as the only unknown. To estimate w' , and thus w , we impose the so-called single-crossing assumption: Suppose that P_1 has more mass in the tails than P_2 , such that for some value \hat{S} it holds

$$\begin{aligned} F_{P_1}(S) &\geq F_{P_2}(S) \quad \forall S \leq \hat{S}, \\ F_{P_1}(S) &\leq F_{P_2}(S) \quad \forall S \geq \hat{S}, \\ F_{P_1}(\hat{S}) &= F_{P_2}(\hat{S}). \end{aligned}$$

Then, Eq. (7) constitutes two Delay Differential Equations (DDE) of neutral type, one DDE for all $S \leq \hat{S}$ and one DDE for all $S \geq \hat{S}$. More precisely, on both subsets, today's derivative of the yet unknown function w depends on its derivative in the past. As a result, we are able to identify $w'(1 - F_{P_2}(S))$ at 'time point' $1 - F_{P_2}(S)$ when 'time point' $1 - F_{P_1}(S)$ lies in the past and $w'(1 - F_{P_1}(S))$ is already known

(and vice versa). Consequently, we can solve the DDE for w' on the two intervals $[0, \hat{S}]$ and $[\hat{S}, \infty)$ and finally, with $w(0) = 0$ and $w(1) = 1$, we identify w .

However, while Dierkes et al. (2022) estimate risk neutral and physical densities from empirically observed option prices, we derive densities from the Pan (2002) model, which we describe in Sect. 2.2. In Sect. 2.3, we provide more details on the estimation of the DDE and outline differences with respect to Dierkes et al. (2022).

2.2 The Pan Pan (2002) model

We obtain risk neutral and physical densities from the Pan (2002) stochastic volatility and jumps model as it offers the advantage that, besides the wealth level, it includes the volatility as an additional state variable, which we can change counterfactually. Note that our analyses are difficult to execute in a nonparametric setup, since—for any given cross-section of option prices—we would not be able to change the volatility state counterfactually without the model framework. At the same time, the Pan (2002) model is rich enough to explain relevant characteristics of S&P 500 index returns and options written on them. Moreover, it provides closed-form expressions for the transforms of both $f_P(S_T)$ and $f_Q(S_T)$, making it appealing for our estimation technique. Given that Polkovnichenko and Zhao (2013) casually observe S-shaped probability weighting functions during times of low volatility and Kilka and Weber (2001) find probability weighting to be more pronounced when agents are less confident in assessing a decision situation, we expect volatility to be an important determinant of probability weighting.⁸

Pan (2002) fits an elaborate model, based on Bates (2000), to S&P 500 option prices and time series of the underlying. More specifically, she proposes a model with stochastic volatility and jumps in the underlying's price process, where jump intensity is correlated with the current level of volatility. The model determines three risk premia: a diffusive (Brownian) risk premium, a volatility risk premium, and a state-dependent jump risk premium. Under the physical measure, Pan (2002) proposes the following process for the underlying index price S_t and variance V_t

$$dS_t = [r_t - q_t + \eta^S V_t + \lambda V_t (\mu - \mu^*)] S_t dt + \sqrt{V_t} S_t dB_t^1 + dZ_t - \mu S_t \lambda V_t dt, \quad (8)$$

$$dV_t = \kappa_v (\bar{v} - V_t) dt + \sigma_v \sqrt{V_t} (\rho dB_t^1 + \sqrt{1 - \rho^2} dB_t^2), \quad (9)$$

where the riskless rate r_t and the dividend yield q_t both follow a square-root process with long-run means \bar{r} and \bar{q} , mean reversion rates κ_r and κ_q , and volatility coefficients σ_r and σ_q , respectively.⁹ Random innovations are introduced by two independent standard Brownian motions, dB_t^1 and dB_t^2 , and a poisson (pure-jump) process, Z_t , whose jump intensity is λV_t and which is thus perfectly correlated with

⁸ In addition to that, several studies relate volatility to the pricing kernel puzzle or risk aversion, e.g. Bliss and Panigirtzoglou (2004), Ziegler (2007), and Linn et al. (2018).

⁹ See Pan (2002)'s Equation (2.3).

the instantaneous variance V_t . The logarithm of the relative jump size, conditional on a jump occurring, is normally distributed with mean $\mu_J = \ln(1 + \mu) - \sigma_J^2/2$ and variance σ_J^2 . Thus, the last term of Eq. (8), $\mu S_t \lambda V_t dt$, compensates for the instantaneous change in expected index returns introduced by the pure-jump process Z_t . The premia for Brownian return risks and jump risks are estimated by $\eta^S V_t$ and $\lambda V_t (\mu - \mu^*)$, respectively. The variance process is modeled by Eq. (9) and follows a square-root process with long-run mean \bar{v} , mean reversion rate κ_v , and volatility σ_v . The Brownian shocks to price S_t and variance V_t are correlated with constant coefficient ρ . Under the risk neutral measure, the dynamics of S_t and V_t evolve according to

$$dS_t = (r_t - q_t)S_t dt + \sqrt{V_t} S_t dB_t^1(Q) + dZ_t^Q - \mu^* S_t \lambda V_t dt, \quad (10)$$

$$dV_t = [\kappa_v(\bar{v} - V_t) + \eta^V V_t] dt + \sigma_v \sqrt{V_t} (\rho dB_t^1(Q) + \sqrt{1 - \rho^2} dB_t^2(Q)), \quad (11)$$

where r_t and q_t are assumed to behave as under the physical measure. $dB_t^1(Q)$, $dB_t^2(Q)$, and Z_t^Q are two independent standard Brownian motions and the poisson (pure-jump) process under the risk neutral measure, respectively. Again, jump intensity is defined by λV_t and the logarithm of the jump size, conditional on a jump occurring, is normally distributed with mean $\mu_J^* = \ln(1 + \mu^*) - \sigma_J^2/2$ and variance σ_J^2 . The variance process in Eq. (11) is defined by the mean reversion rate $\kappa_v^* = \kappa_v - \eta_v$, the long-run mean $\bar{v}^* = \kappa_v \bar{v} / \kappa_v^*$, and the volatility coefficient σ_v . The volatility risk premium is estimated by $\eta^V V_t$.

Pan (2002) estimates parameters with an ‘implied-state’ generalized method of moments (IS-GMM) approach and joint spot and option data from the Berkeley Options Data Base.¹⁰ We provide an overview of the coefficient estimates in Table 1 and employ these to obtain risk neutral and physical densities via Fourier inversion. Thereby, we closely follow Ziegler (2007) and refer to Appendix A for more details.

An obvious concern of our approach is that Pan (2002) applies option data from 1989 to 1996 and the market environment has changed thereafter. In Sect. 4.1, we therefore provide an out-of-sample test by implementing a nonparametric empirical setting for the period from 1996 to 2020. Moreover, in Sect. 4.4 we re-run our simulation with alternative parameters. In both cases, we find our results to hold.

2.3 Differentiation from earlier studies

Although the economic theory underlying our analysis is very similar to that of Dierkes et al. (2022), the actual implementation differs significantly. While they conduct a fully nonparametric approach and obtain risk neutral and physical densities from option prices, we rely on the Pan (2002) model. Our analysis is thus entirely simulation-based. A simulation within this model has clear advantages over

¹⁰ We refer to Pan (2002) for more details.

Table 1 Pan (2002) parameters

Panel A: Pan (2002), Table 3

κ_v	\bar{v}	σ_v	ρ	η^s	η^v	$\lambda^* = \lambda$	μ (%)	σ_J	μ^* (%)
6.4 (1.8)	0.0153 (0.0029)	0.30 (0.04)	-0.53 (0.07)	3.6 (2.4)	3.1 (2.2)	12.3 (1.9)	-0.8 (2.4)	0.0387 (0.0072)	-19.2 (1.8)

Panel B: Pan (2002), Table 6

κ_r	\bar{r}	σ_r	κ_q	\bar{q}	σ_q
0.20 (0.15)	0.058 (0.016)	0.0415 (0.0009)	0.24 (0.33)	0.025 (0.011)	0.0269 (0.0004)

This table presents parameter estimates from the Pan (2002) stochastic volatility and jumps model (see her Tables 3 and 6). Pan (2002) estimates these parameters with an implied-state generalized method of moments (IS-GMM) approach and joint spot and option data from the Berkeley Options Data Base for the period from 1989 to 1996

a nonparametric empirical study. In an empirical study, a variation of volatility can only be observed over time. However, as time proceeds there might also be changes in uncontrolled factors, potentially driving probability weighting, or equivalently, probabilistic risk attitudes. Any empirical study will thus have difficulties in ruling out unobserved variables which drive probability weighting and, coincidentally, correlate with volatility. For example, volatility and, say, sentiment might have changed from month t to month $t + 1$, alongside probability weighting. Then is it difficult to cleanly link the change in probability weighting to the change in volatility. In our present simulation study, based on Pan (2002), we are able to change volatility and, importantly, volatility alone. Furthermore, since probability weighting affects the tails of the underlying's distribution, empirical studies need reliable estimates of those tails. Nonparametric estimates of extreme tails, however, might be contaminated by far out of the money options' illiquidity. The structural nature of a realistically calibrated option pricing model, such as Pan (2002), avoids these pitfalls. Nevertheless, it is reassuring that when we analyze empirical estimates of probability weighting and correlate it with empirically observed volatility, we find results to be consistent with our simulation results (see Sect. 4.1).

To solve the DDE introduced in Sect. 2.1, Dierkes et al. (2022) employ different S&P 500 maturities.¹¹ By repeating this approach each month, they estimate a *time series* of probability weighting functions. We adjust their approach by assuming different levels of volatilities. More specifically, we solve the DDE for volatilities, $v_t = \sqrt{V_t}$, from 0.01 to 0.60 by choosing two adjacent volatility levels, e.g. $v_t = 0.10$ and $v_t + 0.01 = 0.11$. We thus provide a *cross-section* of probability weighting functions, which enables us to investigate the relationship between probability weighting and volatilities.

2.4 Fitting probability weighting functions

Given that we have estimated nonparametric probability weights according to Sects. 2.1 through 2.3, we now have to fit these weights to parametric functions. To do so, we make use of three different functional forms: the two-parameter Prelec (1998) function, the two-parameter linear-in-log-odds function (Tversky and Fox, 1995; Bleichrodt and Pinto, 2000), and the one-parameter Tversky and Kahneman (1992) function, as defined by Eqs. (12), (13), and (14), respectively.

$$w(p) = e^{-\delta(-\log(p))^\gamma}, \quad (12)$$

$$w(p) = \frac{\delta p^\gamma}{\delta p^\gamma + (1-p)^\gamma}, \quad (13)$$

¹¹ We refer to their study for more details. See also Dierkes (2013) who was the first to introduce the elicitation procedure described above.

$$w(p) = \frac{p^\gamma}{(p^\gamma + (1-p)^\gamma)^{1/\gamma}}, \quad (14)$$

where $\gamma < 1$ implies overweighting of small probabilities and the typical inverse S-shape. We estimate δ and γ by fitting Eqs. (12) and (13) with linear regressions according to

$$\log(-\log(w(p))) = \log(\delta) + \gamma \log(-\log(p)) + \epsilon, \quad (15)$$

$$\log\left(\frac{w(p)}{1-w(p)}\right) = \log(\delta) + \gamma \log\left(\frac{p}{1-p}\right) + \epsilon, \quad (16)$$

on the interval $p \in \{0.01, 0.02, \dots, 0.99\}$, while Eq. (14) is fitted with non-linear least squares. ϵ denotes the residuals.

3 Results

3.1 Implied probability weighting functions

In this section, we report results for the main specification of our study, characterized by a return horizon of one year and stochastic volatilities ranging from 0.01 to 0.60. However, in Sect. 4, we show that our results extend to return horizons of three and six months.

In order to estimate implied probability weighting functions, we first obtain physical and risk neutral probabilities according to Sect. 2.2. Figure 1 illustrates the corresponding densities (Panel A) and distribution functions (Panel B) across wealth levels (averaged over volatilities). Dashed lines correspond to 95% point-wise confidence intervals. By construction, our results are very similar to those of Ziegler (2007). This is, the average physical density is located to the right of the risk neutral density and exhibits a more pronounced peak (at a wealth level of 1.13). However, in contrast to Ziegler (2007), we find both densities to be more dispersed and attribute this finding to a different choice of volatilities. While we average over a large set of volatilities, Ziegler (2007)'s results are based on five rather low volatilities, ranging from roughly 0.097–0.145.¹²

In Fig. 2, we illustrate the estimated probability weighting parameters for each volatility level and each of the three functional forms outlined in Sect. 2.4. While we also report the elevation parameter delta (Panel B), we follow Polkovnichenko and Zhao (2013) and focus our analysis on the curvature parameter gamma (Panel A). Although the Pan (2002) model was never designed to match CPT preferences, the relationship between volatilities and probability weighting is strikingly clear. For all weighting functions, probability weighting is present across volatility levels and

¹² Ziegler (2007) bases his choice on the average volatility reported in Pan (2002), i.e. he applies $\bar{v} = \sqrt{0.0153} \pm$ one and two standard errors.

gammas almost monotonically decrease in volatility. This result is well in line with Polkovnichenko and Zhao (2013) and Kilka and Weber (2001). Moreover, it corresponds to Gao et al. (2021) who find that investors dislike high-skewness securities when market volatility is low. With the two-parameter Prelec (1998) specification (γ^{Prelec}), gamma is about 0.99 for very low volatilities and 0.70 for high volatilities. With respect to the linear-in-log-odds function ($\gamma^{Log.Odds}$), our results are very similar as gammas vary from 0.90 to 0.68. In contrast, variation of the Tversky and Kahneman (1992) gamma (γ^{TK92}) is slightly reduced to 0.95 and 0.82, which is likely explained by the fact that the Tversky and Kahneman (1992) function does not include the elevation parameter δ .

In Table 2, we summarize our results and compare them to parameter estimates from previous studies.¹³ Given that Pan (2002) estimates model parameters from the S&P 500, i.e. one of the most liquid and competitive option markets in the world, it is not surprising that our gamma estimates are closer to one compared to, for example, Bleichrodt and Pinto (2000) and Kliger and Levy (2009). However, in line with these studies, we find persistent overweighting of small probabilities, indicating a high demand for lottery-like assets and a large potential impact of probability weighting on the pricing kernel puzzle. Moreover, note that Polkovnichenko and Zhao (2013)'s median estimates (0.90–0.95, depending on the assumed level of risk aversion) are even closer to one. As a result, the average probability weighting function over volatilities (Panel C) is characterized by a pronounced inverse S-shape. According to Polkovnichenko and Zhao (2013), inverse S-shaped probability weighting functions (including a convex segment) are consistent with non-monotonicity in pricing kernels and negative risk aversion functions. As we find pronounced probability weighting, we expect a strong impact of the probabilistic risk attitude on pricing kernels and risk aversion functions.

Apart from that, understanding how probability weighting varies with volatility might help us to understand how negative premia on lottery stocks such as IPOs (Green and Hwang, 2012), SEOs (Chen et al., 2019), and OTC stocks (Eraker and Ready, 2015) change with aggregate volatility. Moreover, M&A activity (Schneider & Spalt, 2017) and the equity share in new issues (Baker & Wurgler, 2000) might also depend on volatility. To quantify the relationship between probability weighting and volatility, we fit linear regressions of gamma on volatilities ($v = 0.01, 0.02, \dots, 0.60$) and variances ($v^2 = 0.01^2, \dots, 0.60^2$). We report the regression estimates below:

$$\begin{aligned}\gamma^{Prelec} &= 0.977 - 1.181v + 1.253v^2, & \text{adj. } R^2 &= 0.978 \\ \gamma^{Log.Odds} &= 0.889 - 0.861v + 0.892v^2, & \text{adj. } R^2 &= 0.980 \\ \gamma^{TK92} &= 0.962 - 0.482v + 0.374v^2, & \text{adj. } R^2 &= 0.989\end{aligned}$$

We conclude that there is a distinct and close relationship between volatility and probability weighting. In times of market distress (when volatility is high), investors

¹³ We refer to Stott (2006) for an extensive overview.

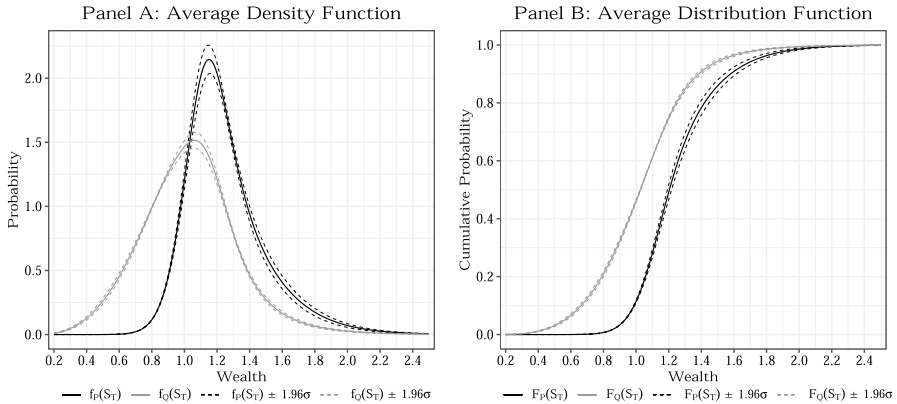


Fig. 1 Physical and risk neutral distributions, 1 year horizon. This figure plots physical and risk neutral densities (Panel A) and distribution functions (Panel B), estimated from the Pan (2002) stochastic volatility and jumps model and averaged over volatilities from 0.01 to 0.60. Physical (risk neutral) densities are denoted by $f_P(S_T)$ ($f_Q(S_T)$), whereas physical (risk neutral) distribution functions are denoted by $F_P(S_T)$ ($F_Q(S_T)$). We assume a return horizon of 1 year

overweight small probabilities and the demand for lottery-like assets increases, while during low volatility regimes weighted probabilities are close to their actual counterparts.

3.2 The pricing kernel puzzle

According to economic theory, the pricing kernel is defined as the ratio of risk neutral to physical probabilities and should monotonically decrease in wealth. The pricing kernel reflects marginal utility of a representative investor and thus implicitly aggregate risk preferences. Put differently, the pricing kernel and risk aversion are two sides of the same coin. A locally decreasing (increasing) pricing kernel directly implies a locally positive (negative) risk aversion and vice versa. Thus, we can make a statement on the pricing kernel either by estimating the pricing kernel itself or by retracing it from risk aversion functions.

However, in contrast to economic theory, several recent studies have captured (locally) U-shaped pricing kernels or negative episodes of the risk aversion function, implying the pricing kernel and risk aversion puzzle, respectively.¹⁴ We tackle these puzzles by adjusting both pricing kernels and risk aversion functions for probability weighting. Note that, although most of our results relate to risk aversion functions, we refer to both puzzles by the term ‘pricing kernel puzzle’ as this term is more frequently used in the literature.

In a first step, we investigate the pricing kernel puzzle by calculating both the raw pricing kernel, i.e. $f_Q(S_T)/f_P(S_T)$, and the pricing kernel net of probability weighting (as outlined in Eq. 1). Recall that the adjusted pricing kernel varies with the physical

¹⁴ See, for example, Jackwerth (2000), Ait-Sahalia and Lo (2000), and Rosenberg and Engle (2002).

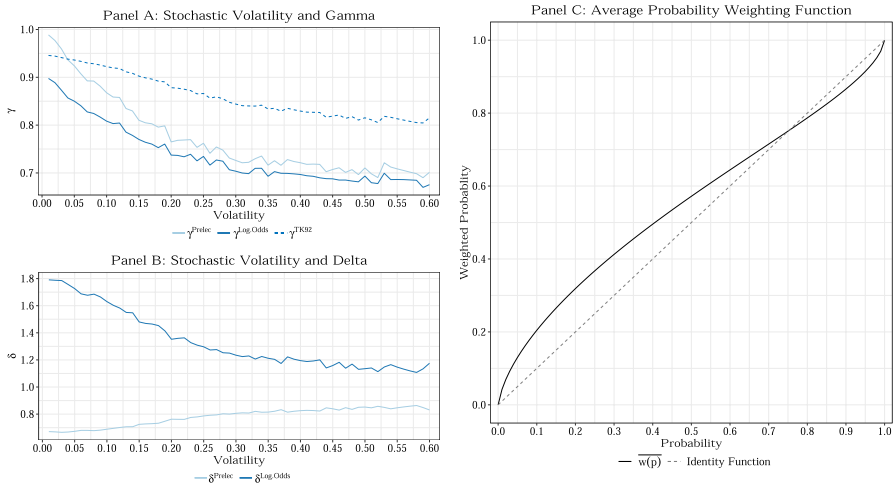


Fig. 2 Implied probability weighting, 1 year horizon. This figure plots results for probability weighting functions estimated from the Pan (2002) stochastic volatility and jumps model. We identify probability weights nonparametrically and estimate parameter values for three well known probability weighting functions, namely the two-parameter weighting function of Prelec (1998), denoted by *Prelec*, the two-parameter linear-in-log-odds function (as used in Tversky and Fox, 1995; Bleichrodt and Pinto, 2000), denoted by *Log.Odds*, and the one-parameter function of Tversky and Kahneman (1992), denoted by *TK92*. While Panel A and Panel B display the curvature parameter γ and the elevation parameter δ , respectively, Panel C shows the probability weighting function averaged over volatilities. We assume a return horizon of 1 year

distribution, $F_p(S_T)$, if the probability weighting function is not linear (i.e. $\gamma \neq 1$). Thus, parts of the probability weighting function with $w'(1 - F_p(S_T)) > 1$ reduce the pricing kernel, whereas parts with $w'(1 - F_p(S_T)) < 1$ increase it. Given our finding of pronounced probability weighting across volatilities, we expect the adjusted pricing kernel to monotonically decrease in wealth.

Figure 3 illustrates both the raw and the adjusted pricing kernel, estimated from the Pan (2002) model and averaged over volatilities. The return horizon is one year and dashed lines correspond to 95% point-wise confidence intervals. Note that, in order to obtain a smooth probabilistic risk attitude, we derive $w'(1 - F_p(S_T))$ and $w''(1 - F_p(S_T))$ analytically by fitting the nonparametric probability weights to the two-parameter weighting function of Prelec (1998). We obtain an almost perfect fit.¹⁵ Consistent with the literature, we find the raw pricing kernel (Panel A) to exhibit a pronounced global U-Shape, implying a decreasing and partially negative risk aversion. Hence, as inferred by Ziegler (2007), the Pan (2002) model alone does not lead to well-behaved preferences. However, by providing closed-form expressions for the transforms of both $f_p(S_T)$ and $f_Q(S_T)$, the model is well-suited to adjust the pricing kernel and risk aversion functions for probability weighting, as outlined by Eqs. (1) and (6). In Panel B, we report results for the adjusted pricing kernel,

¹⁵ Depending on the volatility level, R^2 's vary from 99.74 to 99.99%. The median estimate is 99.96%.

Table 2 Typical parameters of probability weighting functions

Functional form	Study	γ	δ
Prelec	Kliger and Levy (2009)	0.60	0.79
Prelec	Polkovnichenko and Zhao (2013)	0.90–0.95	
Log.Odds	Wu and Gonzalez (1996)	0.68	0.84
Log.Odds	Tversky and Fox (1995)	0.69	0.77
Log.Odds	Bleichrodt and Pinto (2000)	0.55	0.81
Log.Odds	Dierkes et al. (2022)	0.89	
TK92	Tversky and Kahneman (1992)	0.61	
TK92	Wu and Gonzalez (1996)	0.71	
TK92	Zeisberger et al. (2012)	0.86–0.87	
Prelec	This study	0.70–0.99	1.19–1.79
Log.Odds	This study	0.68–0.90	0.68–0.83
TK92	This study	0.82–0.95	

This table lists parameter estimates of previous studies for different probability weighting functions. We report results for the two-parameter weighting function of Prelec (1998), denoted by *Prelec*, the one- and two-parameter linear-in-log-odds function (as used in Tversky and Fox, 1995; Bleichrodt and Pinto, 2000), denoted by *Log.Odds*, and the one-parameter function of Tversky and Kahneman (1992), denoted by *TK92*. We outline these functions in Eqs. (12)–(14), where δ denotes the elevation parameter and γ defines the curvature. The last three rows correspond to our results illustrated in Fig. 2. We report our estimates for the lowest and highest volatility (0.01 and 0.60), respectively. Note that Polkovnichenko and Zhao (2013) apply the two-parameter Prelec (1998) function, but only report median values for the curvature parameter γ . Dierkes et al. (2022) employ the one-parameter linear-in-log-odds function. We only report parameters for gains

which is monotonically decreasing in wealth. Thus, after accounting for probability weighting, the pricing kernel is well in line with economic theory and corresponds to Baele et al. (2019). To have a closer look at the dynamics driving this result, it is natural to investigate risk aversion functions. Fortunately, Eq. (6) enables us to separate risk aversion related to the utility function u (denoted by RRA_u) and risk aversion originating from the probability weighting function w (the probabilistic risk attitude RRA_w).

Figure 4 presents results for a return horizon of 1 year, where risk aversion functions are averaged over volatilities and dashed lines correspond to 95% point-wise confidence intervals. In Panel A, we report the relative risk aversion (RRA) over wealth levels. Risk aversion becomes negative for wealth levels greater than 1.32. By construction, this finding is consistent with Ziegler (2007) and the raw pricing kernel reported in Fig. 3. Moreover, it confirms Campbell and Cochrane (1999) and Brandt and Wang (2003): when the business cycle reaches the trough, wealth levels are low and the corresponding risk aversion is high. Panels B and C illustrate the adjusted risk aversion, RRA_u , and the probabilistic risk attitude, RRA_w , respectively. Most importantly, as RRA_u closely resembles RRA , the adjusted risk aversion is significantly positive and almost constant over wealth levels. Moreover, in accordance with the dynamics outlined in Sect. 2.1, RRA_w is positive and decreasing for low wealth levels, while it becomes negative for wealth levels greater than 1.10. To prove that our findings do not depend on the specific choice of volatilities, we repeat

our calculations for wealth *percentiles* instead of *levels* and present results in Panels D to F.¹⁶ In fact, the high risk aversion for wealth levels smaller than 0.80 appears to be driven by only a few wealth percentiles. However, the probabilistic risk attitude, RRA_w , still resembles this behavior very closely, resulting in a positive and almost constant adjusted risk aversion, RRA_w .¹⁷ Again, this is a surprisingly clear result given that the Pan (2002) model does not account for probability weighting. However, a reasonable concern of our approach is that we calculate $w'(1 - F_p(S_T))$ and $w''(1 - F_p(S_T))$ analytically by fitting the estimated probability weights to the weighting function of Prelec (1998). In Sect. 4.3, we accommodate this concern by providing results for both an alternative functional assumption and a numerical solution.

Our results shed further light on the dynamics driving the pricing kernel puzzle. By accounting for probability weighting, we obtain a monotonically decreasing pricing kernel and a decreasing but consistently positive risk aversion. Importantly, we show that negative episodes of the risk aversion function arise due to the probabilistic risk attitude being negative for high wealth levels. We thus conclude that the probabilistic risk attitude is a promising explanation for the pricing kernel puzzle.

4 Robustness

4.1 Empirical relationship between probability weighting and volatility

While our main results are based on the Pan (2002) model and suggest a strongly negative relation between gamma and stochastic volatility (i.e. probability weighting increases in volatility), it is reasonable to ask whether this relationship extends to a nonparametric empirical setting. We therefore follow Dierkes et al. (2022) and utilize a time series of monthly gammas from nonparametric estimates of the physical density function f_p (via S&P 500 returns) and the risk neutral density f_Q (via S&P 500 option prices).¹⁸ To measure volatility, we employ the option-implied volatility index *VIX* which is provided by the Chicago Board Options Exchange (CBOE) on a daily basis. To reconcile both time series, we calculate the monthly average of daily *VIX* closing prices. Data on gammas is provided by Dierkes et al. (2022). Due to data availability, we cover a sample period from February 1996 to December 2020. As this period directly follows the sample period used in Pan (2002), our robustness check also serves as an out-of-sample test.

Most importantly, we once more find a strongly negative relationship. For example, a univariate regression of gamma on the *VIX* yields a negative and highly

¹⁶ For example, low volatilities correspond to almost no probability mass for wealth levels greater than 1.40.

¹⁷ Note that risk aversion estimates become insignificant for the lowest wealth percentiles as there is a strongly increased standard deviation.

¹⁸ The authors illustrate that their measure closely reflects several stock market episodes like the Dot-Com bubble, the subprime crisis, and the recent surge in lottery demand in 2020 and 2021 (see their Fig. 1). Parameters are fitted based on the two-parameter log-odds function.

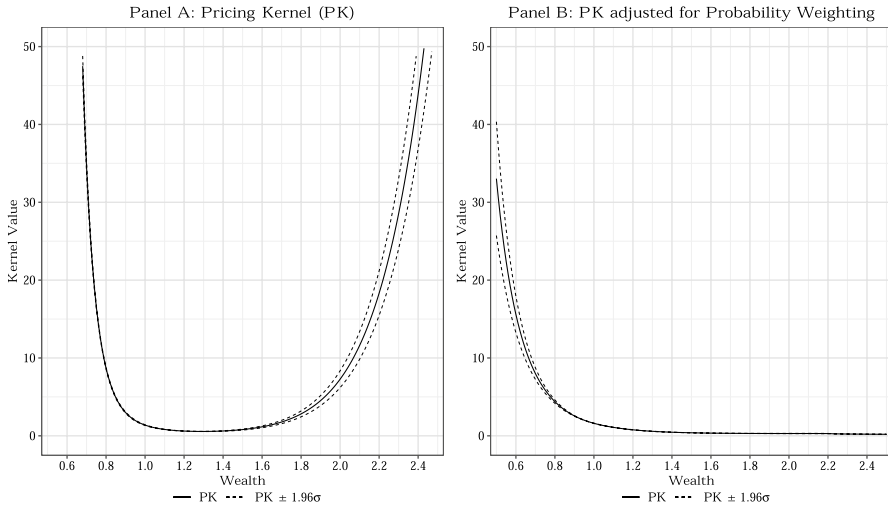


Fig. 3 Average pricing kernel, 1 year horizon. This figure plots pricing kernels estimated from the Pan (2002) stochastic volatility and jumps model. Following the literature (e.g. Jackwerth, 2000, Baele et al., 2019), we estimate the pricing kernel (PK, Panel A) as the ratio of the risk neutral to the physical probabilities, i.e. $PK = f_Q/f_P$. In Panel B, we follow Eq. (1) and calculate the pricing kernel, net of probability weighting, as $PK = f_Q(S_T)/f_P(S_T) \cdot w'(1 - F_P(S_T))$. We assume a return horizon of 1 year

significant coefficient estimate ($t = -10.91$) and $R^2 = 28.4\%$. By including an additional variance term (as in Sect. 3.1), R^2 even increases to 30.1%. Moreover, the difference between average gammas in high (0.71) and low volatility regimes (1.06), according to a median split of the *VIX*, is economically important and statistically significant at the 1%-level ($t = -8.05$).

In Fig. 5, we illustrate the empirical link between probability weighting and volatilities by estimating the lowess-smoothed relationship between gamma and the *VIX*. The range of gammas increases, yet the shape of the smoothed relationship is surprisingly close to that reported in Panel A of Fig. 2. First, gamma monotonically decreases in volatility, indicating more pronounced probability weighting in volatile market environments. Second, gamma strongly decreases for low *VIX* levels, while the slope is less steep for volatilities greater than 0.35, suggesting that the differential impact is stronger in low volatility periods.¹⁹ The empirical relationship is thus well in line with Kilka and Weber (2001) and Gao et al. (2021) and confirms our simulation-based conclusions.

In Fig. 6, we compare the monthly empirical gammas (Panel A) to a time series of gammas implied by our simulation approach (Panel B). In order to estimate the model-implied gammas, we employ the monthly average of daily *VIX* closing prices and match each value according to the relationship presented in Fig. 2.

¹⁹ Replacing the average *VIX* by the maximum *VIX* per month leads to very similar results. However, while maintaining its shape, the lowess-smoothed relationship is, by construction, slightly shifted upwards.

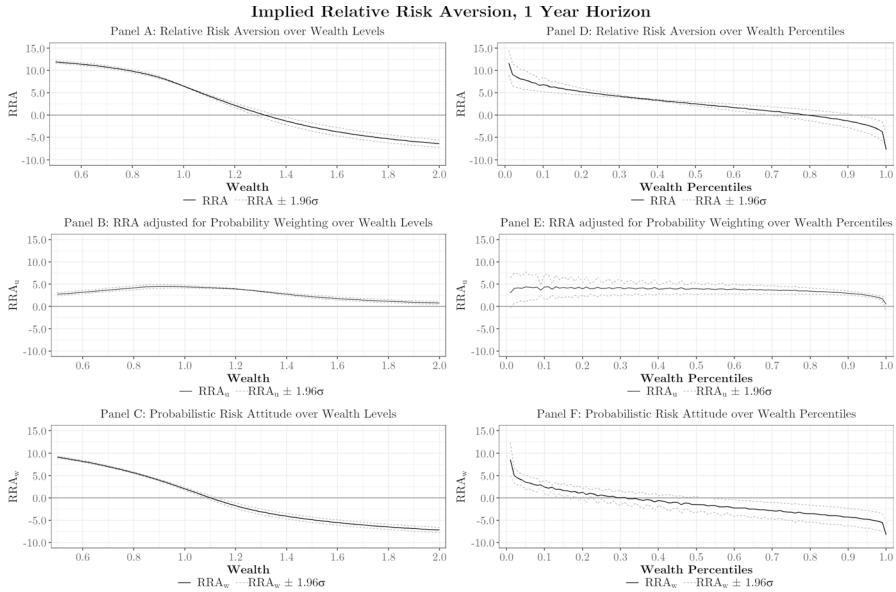


Fig. 4 Implied relative risk aversion, 1 year horizon. This figure plots implied risk aversion functions estimated from the Pan (2002) stochastic volatility and jumps model. In Panel A, we report the relative risk aversion (RRA) over wealth levels, averaged across volatilities from 0.01 to 0.60 and calculated as $RRA = S_T (F'_p(S_T)/F_p(S_T) - F'_Q(S_T)/F_Q(S_T))$. In Panel B, we report RRA functions adjusted for the probabilistic risk attitude (as outlined by Eq. 6), i.e. $RRA_u = RRA - S_T \frac{w''(1-F_p(S_T))}{w'(1-F_p(S_T))} \cdot f_p(S_T)$. We derive $w''(1 - F_p(S_T))$ and $w'(1 - F_p(S_T))$ analytically by fitting the nonparametrically estimated probability weights to the two-parameter probability weighting function of Prelec (1998). In Panels D to F, we repeat all estimations for wealth percentiles instead of wealth levels. We assume a return horizon of 1 year

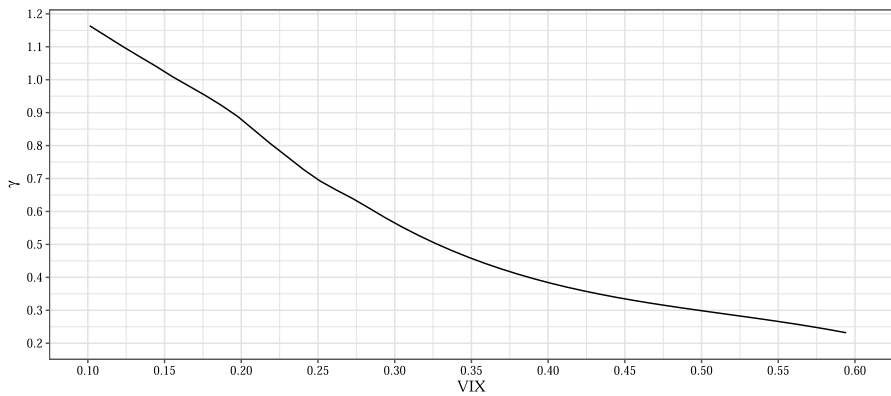


Fig. 5 Empirical relationship between probability weighting and volatility. This figure plots the lowest-smoothed empirical relationship between the probability weighting parameter gamma and volatility. Gammas are estimated by applying nonparametric estimates of the physical density function f_p (via S&P 500 returns) and the risk neutral density f_Q (via S&P 500 option prices), while volatilities are proxied by the option-implied volatility index VIX . As data on the VIX is provided on a daily basis, we employ the monthly average of daily VIX closing prices. Due to data availability, we cover a sample period from February 1996 to December 2020

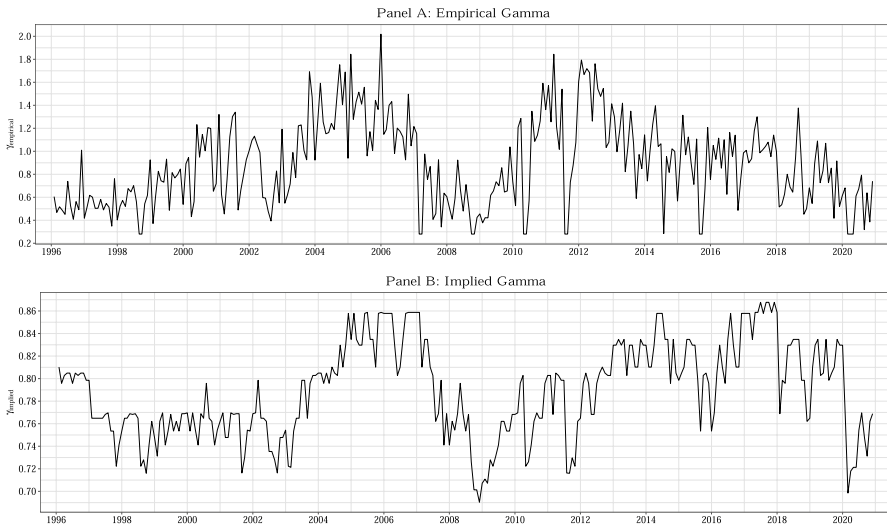


Fig. 6 Empirical and model-implied probability weighting. Panel A of Fig. 6 plots the time series of empirical gammas as described in Fig. 5. Panel B illustrates a time series of model-implied gammas. In order to estimate this time series, we employ the monthly average of daily VIX closing prices and match each value according to the relationship presented in Fig. 2. Due to data availability, we cover a sample period from February 1996 to December 2020

While model-implied gammas are, by construction, more condensed, the overall shape of both time series is remarkably close. For example, both time series display lower gammas (i.e. increased probability weighting) during the run-up of the DotCom bubble in 1998–2000 and the subprime crisis in 2007–2009. Moreover, both estimates nicely reflect increased probability weighting after Covid-19 reached global stock markets in March 2020. In line with this, we also find a large correlation between the two time series (54.5%). We therefore consider our results as further out-of-sample evidence. Moreover, they are well in line with the literature on time-varying risk preferences, e.g. Brandt and Wang (2003), Guiso et al. (2018), and Polkovnichenko and Zhao (2013).

While it is reassuring that the empirical results confirm our simulation-based findings, note that in such an exercise it is not possible to counterfactually change the volatility level with all else being equal. That is, an analysis using several months with varying volatility could have been confounded by additional time-varying economic state variables. This is why, in our baseline analysis, we opted for model-based results with volatility as the only additional state variable.

4.2 Alternative maturities

To prove that our results hold for alternative assumptions, we now repeat our estimations for return horizons of 6 and 3 months and focus on the most important components: volatility-dependent probability weighting and the impact of the

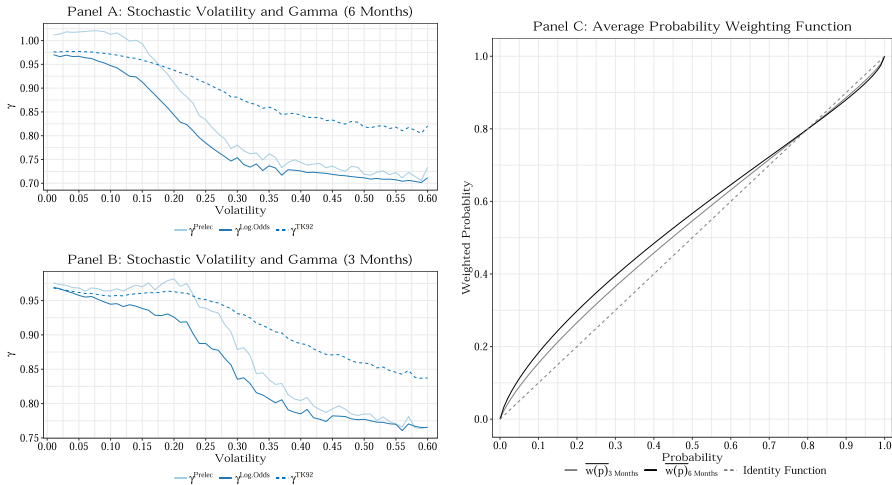


Fig. 7 Implied probability weighting, 6 months and 3 months horizon. This figure plots results for probability weighting functions estimated from the Pan (2002) stochastic volatility and jumps model. We identify probability weights nonparametrically and estimate parameter values for three well known probability weighting functions, namely the two-parameter weighting function of Prelec (1998), denoted by *Prelec*, the two-parameter linear-in-log-odds function (as used in Tversky and Fox, 1995; Bleichrodt and Pinto, 2000), denoted by *Log.Odds*, and the one-parameter function of Tversky and Kahneman (1992), denoted by *TK92*. While Panel A and Panel B display the curvature parameter γ for a return horizon of six and three months, respectively, Panel C shows the probability weighting function averaged over volatilities. We assume a return horizon of 6 months

probabilistic risk attitude on risk aversion functions. However, we report corresponding risk neutral and physical densities as well as pricing kernels in Appendices B and C, respectively.

Figure 7 illustrates the curvature parameter gamma as well as the average probability weighting function for return horizons of six and three months, respectively. With respect to a return horizon of six months (Panel A), the variation in gamma is very similar to our main specification. While γ^{Prelec} varies from 1.02 for low volatilities to 0.71 for high volatilities, $\gamma^{Log.Odds}$ decreases from roughly 0.97–0.70. Notably, γ^{Prelec} is rather constant for volatilities between 0.01 and 0.11 and then sharply decreases for volatilities between 0.12 and 0.30. Again, the variation in γ^{TK92} is somewhat smaller (0.98–0.80) but still reasonable. Most importantly, even though gammas seem to be shifted upwards, we still find a strongly negative relationship with volatilities. As a result, the average probability weighting function (black solid line in Panel C) displays a distinct, but slightly less pronounced, inverse S-shape. Panel B reports gammas for a return horizon of three months. γ^{Prelec} ($\gamma^{Log.Odds}$) now varies from roughly 0.98–0.77 (0.97–0.78), whereas γ^{TK92} ranges from 0.97 to 0.84. Again, γ^{Prelec} is almost constant for small volatilities and then sharply decreases. Although gammas are below one, the overall level is further shifted upwards. As a consequence, the average probability weighting function (grey solid line in Panel C) is closer to the identity function (dashed line), but still preserves an inverse S-shape.

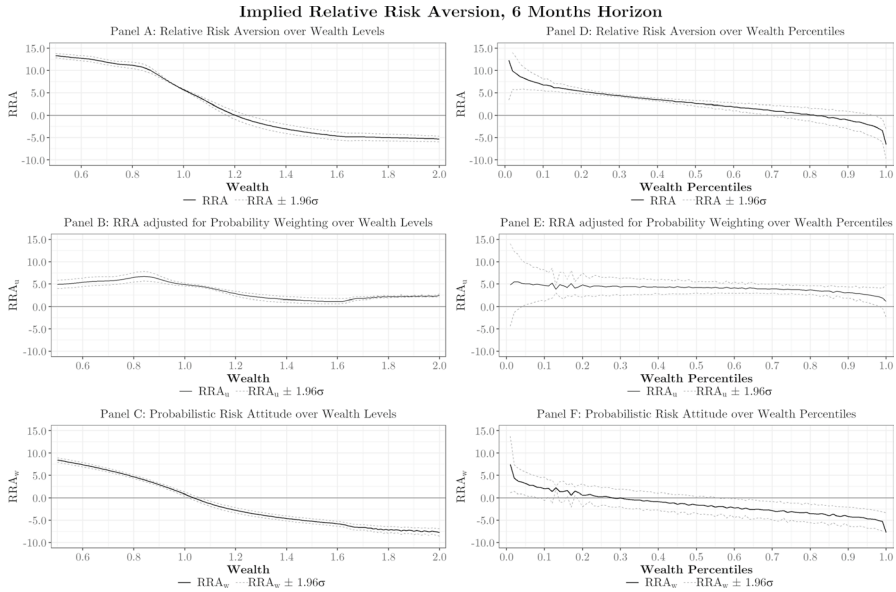


Fig. 8 Implied relative risk aversion, 6 months horizon. This figure plots implied risk aversion functions estimated from the Pan (2002) stochastic volatility and jumps model. In Panel A, we report the relative risk aversion (RRA) over wealth levels, averaged across volatilities from 0.01 to 0.60 and calculated as $RRA = S_T (F'_p(S_T)/F_p(S_T) - F'_Q(S_T)/F_Q(S_T))$. In Panel B, we report RRA functions adjusted for the probabilistic risk attitude (as outlined by Eq. 6), i.e. $RRA_u = RRA - S_T \frac{w''(1-F_p(S_T))}{w'(1-F_p(S_T))} \cdot f_p(S_T)$. We derive $w''(1 - F_p(S_T))$ and $w'(1 - F_p(S_T))$ analytically by fitting the estimated probability weights to the two-parameter probability weighting function of Prelec (1998). In Panels D to F, we repeat all estimations for wealth percentiles instead of wealth levels. We assume a return horizon of 6 months

We thus conclude that the estimation of probability weights is robust to alternative return horizons.

To further investigate the pricing kernel puzzle, we focus on the adjusted risk aversion (RRA_u). Figure 8 illustrates risk aversion functions for a return horizon of six months. In Panel A, we report the average risk aversion over wealth levels. While the overall shape is close to our main specification, RRA is slightly shifted upwards and becomes negative for wealth levels greater than 1.20 (compared to 1.32 for a return horizon of one year). In contrast to Fig. 4, the adjusted risk aversion, RRA_u , is somewhat bumpier and slightly increasing for wealth levels greater than 1.60 (with very little probability mass, Panel B). Most importantly, RRA_u remains significantly positive for all wealth levels and thus implies a monotonically decreasing pricing kernel. The probabilistic risk attitude is almost unchanged, i.e. RRA_w is positive and decreasing for low wealth levels, and negative for wealth levels greater than 1.05 (Panel C). With respect to wealth percentiles (Panels D to F), results correspond to our main specification. Notably, except for some noise around the 15% quantile, there are no episodes of increasing RRA_u . We therefore argue that increasing segments in Panel B are merely an artifact of averaging over volatilities.

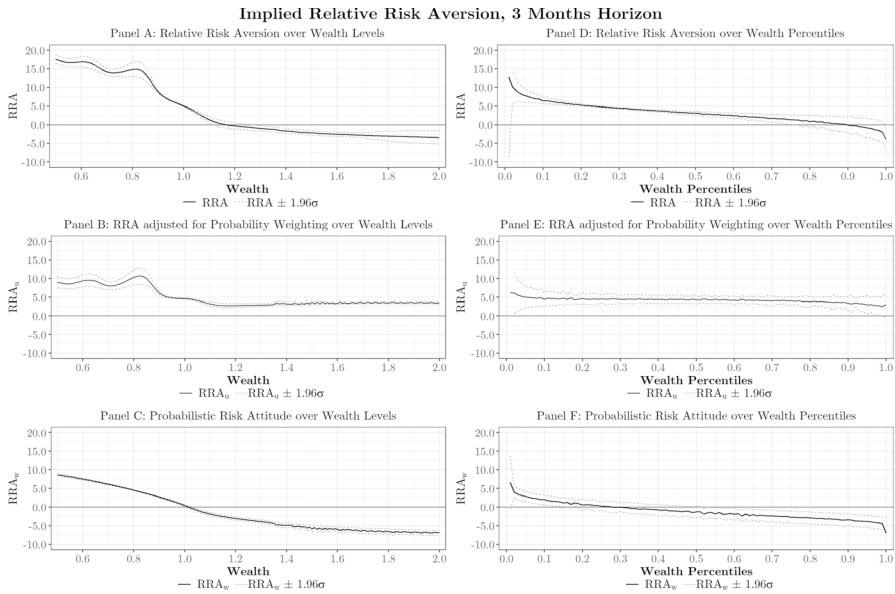


Fig. 9 Implied relative risk aversion, 3 months horizon. This figure plots implied risk aversion functions estimated from the Pan (2002) stochastic volatility and jumps model. In Panel A, we report the relative risk aversion (RRA) over wealth levels, averaged across volatilities from 0.01 to 0.60 and calculated as $RRA = S_T \left(F'_p(S_T)/F_p(S_T) - F'_Q(S_T)/F_Q(S_T) \right)$. In Panel B, we report RRA functions adjusted for the probabilistic risk attitude (as outlined by Eq. 6), i.e. $RRA_u = RRA - S_T \frac{w''(1-F_p(S_T))}{w'(1-F_p(S_T))} \cdot f_p(S_T)$. We derive $w''(1 - F_p(S_T))$ and $w'(1 - F_p(S_T))$ analytically by fitting the nonparametrically estimated probability weights to the two-parameter probability weighting function of Prelec (1998). In Panels D to F, we repeat all estimations for wealth percentiles instead of wealth levels. We assume a return horizon of 3 months

Figure 9 illustrates results for a return horizon of 3 months. In contrast to our main specification, RRA is shifted upwards and appears to be more bumpy. However, RRA still strongly decreases in wealth. Since the probabilistic risk attitude is only slightly affected, the bumpy shape of RRA directly transfers to the adjusted risk aversion. Hence, RRA_u exhibits increasing parts around a wealth level of 0.80 (with a physical density of almost zero). Most importantly, RRA_u is consistently positive and Panel E confirms that increasing episodes are, again, an artifact of averaging over volatilities.

In summary, we find our results to be robust to alternative maturities. Although risk aversion functions are less smooth, we find the risk aversion—net of probability weighting—to remain significantly positive over both wealth levels and wealth percentiles, implying a monotonically decreasing pricing kernel.

4.3 Alternative estimation of the probabilistic risk attitude

A natural concern of our approach is that we derive $w'(1 - F_p(S_T))$ and $w''(1 - F_p(S_T))$ analytically by fitting nonparametric probability weights to the two-parameter function of Prelec (1998). Thus, our results might reflect the specific

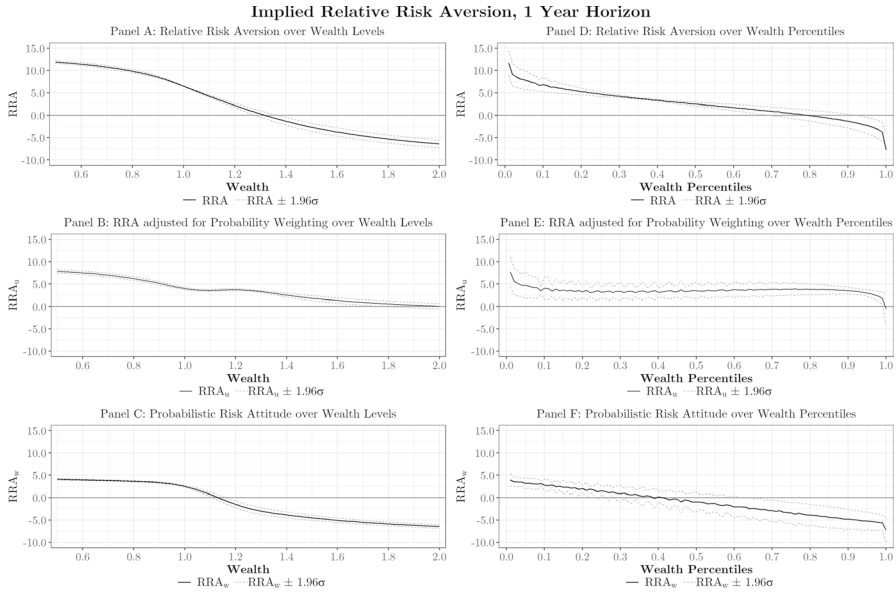


Fig. 10 Implied relative risk aversion, linear-in-log-odds, 1 year horizon. This figure plots implied risk aversion functions estimated from the Pan (2002) stochastic volatility and jumps model. In Panel A, we report the relative risk aversion (RRA) over wealth levels, averaged across volatilities from 0.01 to 0.60 and calculated as $RRA = S_T \left(F'_P(S_T)/F_P(S_T) - F'_Q(S_T)/F_Q(S_T) \right)$. In Panel B, we report RRA functions adjusted for the probabilistic risk attitude (as outlined by Eq. 6), i.e. $RRA_u = RRA - S_T \frac{w''(1-F_P(S_T))}{w'(1-F_P(S_T))} \cdot f_P(S_T)$. We derive $w''(1 - F_P(S_T))$ and $w'(1 - F_P(S_T))$ analytically by fitting the nonparametrically estimated probability weights to the two-parameter linear-in-log-odds probability weighting function (Tversky and Fox, 1995; Bleichrodt and Pinto, 2000). In Panels D to F, we repeat all estimations for wealth percentiles instead of wealth levels. We assume a return horizon of 1 year

functional assumption. To accommodate this concern, we first replace our functional assumption by the linear-in-log-odds probability weighting function and then provide an entirely numerical solution. Results for the linear-in-log-odds function and a return horizon of one year are presented in Fig. 10.²⁰

By construction, relative risk aversion functions in Panels A and D are not affected by a change of the functional assumption since RRA does not depend on $w'(1 - F_P(S_T))$ or $w''(1 - F_P(S_T))$. Hence, changes in RRA_u (Panels B and E) solely depend on RRA_w (Panels C and F). In contrast to our main specification, we find the probabilistic risk attitude to be less pronounced for low wealth levels.²¹ Thus, for a wealth level of 0.50, we find $RRA_u \approx 8$, whereas in our main specification it holds $RRA_u \approx 3$. Most importantly, RRA_u remains positive throughout wealth levels and all but the highest wealth percentile, again implying a monotonically decreasing

²⁰ Again, we find an almost perfect fit.

²¹ See Dierkes and Sejdiu (2019) for differences in the probabilistic risk attitude of various probability weighting functions for probabilities near zero.

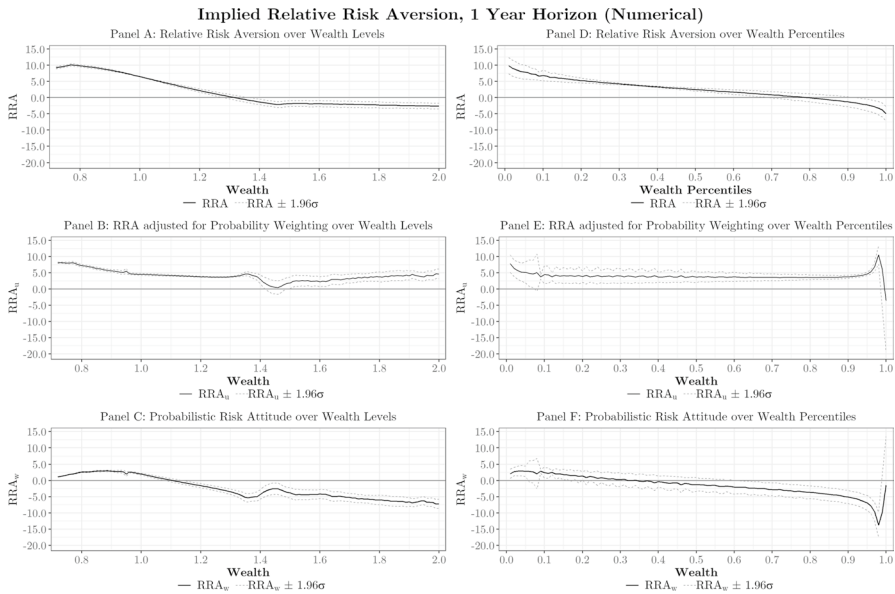


Fig. 11 Implied Relative Risk Aversion, Numerical Solution, 1 Year Horizon. This figure plots implied risk aversion functions estimated from the Pan (2002) stochastic volatility and jumps model. In Panel A, we report the relative risk aversion (RRA) over wealth levels, averaged across volatilities from 0.01 to 0.60 and calculated as $RRA = S_T \left(F'_p(S_T)/F_p(S_T) - F'_Q(S_T)/F_Q(S_T) \right)$. In Panel B, we report RRA functions adjusted for the probabilistic risk attitude (as outlined by Eq. 6), i.e. $RRA_u = RRA - S_T \frac{w''(1-F_p(S_T))}{w'(1-F_p(S_T))} \cdot f_p(S_T)$. In contrast to our main specification, we derive $w''(1 - F_p(S_T))$ and $w'(1 - F_p(S_T))$ numerically. In Panels D to F, we repeat all estimations for wealth percentiles instead of wealth levels. We assume a return horizon of one year

pricing kernel. Moreover, except for some noise, RRA_u is monotonically decreasing. Even though RRA_u is not significant for wealth levels greater than 1.77, it should again be noted that there is only little probability mass for these wealth levels (see Fig. 1). We therefore conclude that our findings are robust to a different functional assumption.

In Fig. 11, we present the resulting risk aversion functions when $w'(1 - F_p(S_T))$ and $w''(1 - F_p(S_T))$ are derived numerically, i.e. without fitting probability weights to a parametric weighting function. A word of caution is in order. As mentioned in Sect. 2.4, we estimate probability weights on the interval $p \in \{0.01, 0.02, \dots, 0.99\}$. Hence, we are not able to estimate probability weights unless it holds for at least one volatility that $F_p(S_T) \geq 0.01$ or $F_p(S_T) \leq 0.99$. Moreover, to derive $w'(1 - F_p(S_T))$ and $w''(1 - F_p(S_T))$ numerically, we lose two more observations. We therefore propose a fine grid for the two probabilities at the extremes and a regular grid in between, i.e. $p \in \{0.001, 0.002, 0.01, 0.02, \dots, 0.99, 0.998, 0.999\}$. By this means, we obtain the probabilistic risk attitude for at least one volatility and wealth levels between 0.72 and 2.00. Consequently, Fig. 11 is also limited to this range.

In Panel A, we report the relative risk aversion which is slightly increasing for wealth levels below 0.78 and greater than 1.47. Note that, even though RRA does

not depend on $w'(1 - F_p(S_T))$ or $w''(1 - F_p(S_T))$, the function differs from Figs. 4 and 10. The rationale is given by the fact that for wealth levels below 0.78 and above 1.47, $w'(1 - F_p(S_T))$ and $w''(1 - F_p(S_T))$ are only known for *some* of the examined volatilities. For wealth levels *between* 0.78 and 1.47, RRA is equal to Fig. 4. Resulting from the estimation instabilities described above, the probabilistic risk attitude is less smooth and locally increasing (Panel C). Nevertheless, we find the global shape, i.e. $RRA_w > 0$ for small wealth levels and $RRA_w < 0$ for high wealth levels, to be preserved. As a consequence, RRA_u remains significantly positive for the vast majority of wealth levels (Panel B). Panels D to F present results for wealth percentiles. Except for the highest wealth percentile, RRA_u is consistently positive and significant throughout the vast majority of wealth percentiles.

Even though the estimation procedure is less stable, our results are thus robust to a numerical solution. In unreported results, we repeat our calculations for return horizons of three and six months and find our conclusions to hold.²²

4.4 Sensitivity analysis

Our simulation approach is not only based on the Pan (2002) model, but also relies on the corresponding parameter estimates. Although results in Sect. 4.1 hint that our findings related to gamma extend to the 1996–2020 period, a reasonable concern of our approach is that Pan (2002) employed options data from 1989 to 1996 and the market environment has changed thereafter. Below, however, we show that this concern is not warranted as we re-run our simulation with alternative parameters. More precisely, we adjust each parameter for \pm one standard error ($\hat{\sigma}_{SE}$) and summarize results in Table 3.²³

We find our results to be remarkably robust. For example, variation in parameters related to the interest rate r and the dividend yield q does not involve any considerable impact on probability weighting and risk aversion functions. Moreover, our conclusions remain unaffected by variation in the jump risk premium $\lambda V_i(\mu - \mu^*)$, the volatility coefficient σ_v , and the correlation between Brownian shocks ρ . Nevertheless, there are some minor instabilities which we want to outline hereafter.

Considering the mean reversion rate of the variance process, $\hat{\kappa}_v - 1\hat{\sigma}_{SE}$ results in an increasing gamma for volatility levels greater than 0.50. The average probability weighting function, however, is still strongly inverse S-shaped and RRA_u is not affected. With respect to the average volatility, we find that $\hat{v} - 1\hat{\sigma}_{SE}$ results in an unstable estimation of the DDE for $v > 0.45$. Moreover, RRA_u is positive but not significant for wealth levels greater than 1.75 (with a corresponding probability mass of below 1%). In case of $\hat{\eta}^S + 1\hat{\sigma}_{SE}$ (related to the premium for Brownian risk), estimating the DDE becomes numerically unstable for $v > 0.53$ and gamma increases

²² Confidence intervals in the numerical solution tend to increase. However, RRA_u remains significantly positive for the vast majority of wealth levels and percentiles.

²³ We thereby assume the remaining parameters to be constant. Strictly speaking, a changed market environment will also result in different standard errors. However, given our results in Sect. 4.1, we assume sufficient accuracy.

Table 3 Sensitivity analysis

Parameter	Estimate (Std. Error)	Comments
Panel A: Pan (2002), Table 3		
κ_v	6.4 (1.8)	In case of $\hat{\kappa}_v - 1\hat{\sigma}_{SE}$, gamma increases for $\sqrt{V} > 0.50$. Probability weighting remains strongly inverse S-shaped.
\bar{v}	0.0153 (0.0029)	In case of $\hat{v} - 1\hat{\sigma}_{SE}$, our code becomes numerically unstable for $\sqrt{V} > 0.45$. $RRA_u > 0$, but not significant for wealth levels > 1.75 (probability mass is below 1%).
σ_v	0.30 (0.04)	
ρ	-0.53 (0.07)	
η^s	3.6 (2.4)	In case of $\hat{\eta}^s + 1\hat{\sigma}_{SE}$, our code becomes numerically unstable for $\sqrt{V} > 0.53$ and gamma increases for $\sqrt{V} > 0.43$. Probability weighting remains strongly inverse S-shaped.
η^v	3.1 (2.2)	In case of $\hat{\eta}^v - 1\hat{\sigma}_{SE}$, even RRA is always positive. In case of $\hat{\eta}^v + 1\hat{\sigma}_{SE}$, RRA (and also RRA_w) are strongly negative for higher wealth levels. RRA_u is moderately negative for wealth levels > 1.50 . RRA_u over wealth percentiles, however, remains positive for all but the highest percentile.
$\lambda^* = \lambda$	12.3 (1.9)	
μ (%)	-0.8 (2.4)	
σ_J	0.0387 (0.0072)	In case of $\hat{\sigma}_J + 1\hat{\sigma}_{SE}$, our code becomes numerically unstable for $\sqrt{V} > 0.48$. Numerically derived RRA_u is < 0 for wealth levels > 1.92 (corresponding probability mass is almost zero).
μ^* (%)	-19.2 (1.8)	
Panel B: Pan (2002), Table 6		
κ_r	0.20 (0.15)	
\bar{r}	0.058 (0.016)	
σ_r	0.0415 (0.0009)	
κ_q	0.24 (0.33)	
\bar{q}	0.025 (0.011)	
σ_q	0.0269 (0.0004)	

This table presents parameter estimates from the Pan (2002) stochastic volatility and jumps model (see her Tables 3 and 6). To check whether our results are robust to variations of these parameters, we re-run our calculations with $\pm 1\hat{\sigma}_{SE}$. While \sqrt{V} indicates volatilities, RRA , RRA_u , and RRA_w denote the relative risk aversion, adjusted risk aversion (related to the utility function), and the probabilistic risk attitude, respectively. We assume a return horizon of 1 year and derive $w''(1 - F_p(S_T))$ and $w'(1 - F_p(S_T))$ analytically by fitting nonparametrically estimated probability weights to the two-parameter probability weighting function of Prelec (1998)

for $v > 0.43$. Nevertheless, probability weighting remains strongly inverse S-shaped. The largest impact on our results is given by a variation of the variance risk premium $\hat{\eta}^v$. In case of $\hat{\eta}^v - 1\hat{\sigma}_{SE}$, even RRA is consistently positive, while for $\hat{\eta}^v + 1\hat{\sigma}_{SE}$ both RRA and the probabilistic risk attitude are strongly negative. As a result, RRA_u is slightly negative for wealth levels greater than 1.50. Importantly, RRA_u over wealth percentiles remains positive for all but the highest percentile. Finally, variation in the jump size volatility ($\hat{\sigma}_J + 1\hat{\sigma}_{SE}$) causes the DDE to become unstable for

$\nu > 0.48$. Despite that, our conclusions with respect to RRA_{it} and probability weighting functions remain unaffected.

In summary, we find some specifications for which solving the DDE becomes numerically unstable in case of large volatilities. Our conclusions, however, remain largely unaffected. We still find a strongly negative (positive) relationship between volatility and gamma (probability weighting), and after accounting for probability weighting, risk aversion functions are mostly significantly positive. Lastly, note that volatilities greater than 0.50 only occur with a probability of less than one percent.²⁴

5 Concluding remarks

We contribute to a large body of literature on time-varying risk preferences and the pricing kernel puzzle. Following Ziegler (2007), we obtain risk neutral and physical densities from the Pan (2002) stochastic volatility and jumps model for a large set of volatilities. Thereafter, we employ these densities to estimate nonparametric probability weights, which we fit to three well-known probability weighting functions: the two-parameter Prelec (1998) function, the two-parameter linear-in-log-odds function, and the one-parameter Tversky and Kahneman (1992) function. Even though the Pan (2002) model was not designed to account for CPT preferences, our results are strikingly clear. Implied probability weighting functions are strongly inverse S-shaped and the curvature parameter gamma almost monotonically decreases in volatility, suggesting that skewness preferences are more pronounced in volatile market environments. Moreover, we estimate probabilistic risk attitudes, equivalent to the share of risk aversion related to probability weighting. In doing so, we fit the estimated probability weights to the functional assumption of Prelec (1998) and calculate derivatives analytically. This enables us to adjust pricing kernel and risk aversion functions for probability weighting and to shed further light on the pricing kernel puzzle. We find the raw pricing kernel, implied by the Pan (2002) model, to display a pronounced U-shape, implying episodes of negative risk aversion. After taking into account probability weighting, however, the pricing kernel is monotonically decreasing in wealth and risk aversion functions remain significantly positive. Our results are robust to alternative return horizons, wealth percentiles, an alternative functional assumption and both a numerical approach to estimate the probabilistic risk attitude and variations of the Pan (2002) coefficient estimates. Moreover, we provide an out-of-sample test by implementing a nonparametric empirical setting for the period from 1996 to 2020, confirming that Pan (2002)'s parameter estimates are still appropriate. We therefore conclude that probability weighting is not only closely related to volatile market environments, but is also a key driver of the pricing kernel puzzle.

²⁴ Given daily VIX closing prices from January 1990 to August 2022, the probability for volatilities greater than 0.50 (0.45) is 0.90% (1.36%).

Appendix A: estimation of physical and risk neutral densities

To estimate physical and risk neutral densities, we closely follow Ziegler (2007) who provides time- t conditional Fourier transforms of $\ln(S_T)$.²⁵ Given the notation outlined in Sect. 2.2 and initial values for the interest rate r , the dividend yield q , the volatility v , and the return horizon $\tau = T - t$, Ziegler (2007) provides the time- t conditional transform under the physical measure as

$$\psi(S; v, r, q, \tau) = \exp(\alpha_r(S) + \alpha_q(S) + \alpha_v(S) + \beta_r(S)r + \beta_q(S)q + \beta_v(S)v), \quad (17)$$

where α_i and β_i ($i = r, q, v$) are defined as

$$\alpha_r = -\frac{\kappa_r \bar{r}}{\sigma_r^2} \left((\gamma_r - \kappa_r) \tau + 2 \ln \left(1 - (\gamma_r - \kappa_r) \frac{1 - \exp(-\gamma_r \tau)}{2\gamma_r} \right) \right), \quad (18)$$

$$\alpha_q = -\frac{\kappa_q \bar{q}}{\sigma_q^2} \left((\gamma_q - \kappa_q) \tau + 2 \ln \left(1 - (\gamma_q - \kappa_q) \frac{1 - \exp(-\gamma_q \tau)}{2\gamma_q} \right) \right), \quad (19)$$

$$\alpha_v = -\frac{\kappa_v \bar{v}}{\sigma_v^2} \left((\gamma_v + b) \tau + 2 \ln \left(1 - (\gamma_v + b) \frac{1 - \exp(-\gamma_v \tau)}{2\gamma_v} \right) \right), \quad (20)$$

$$\beta_r = -\frac{2(1-S)(1 - \exp(-\gamma_r \tau))}{2\gamma_r - (\gamma_r - \kappa_r)(1 - \exp(-\gamma_r \tau))}, \quad (21)$$

$$\beta_q = -\frac{2S(1 - \exp(-\gamma_q \tau))}{2\gamma_q - (\gamma_q - \kappa_q)(1 - \exp(-\gamma_q \tau))}, \quad (22)$$

$$\beta_v = -\frac{a(1 - \exp(-\gamma_v \tau))}{2\gamma_v - (\gamma_v + b)(1 - \exp(-\gamma_v \tau))}, \quad (23)$$

with

$$\gamma_r = \sqrt{\kappa_r^2 + 2(1-S)\sigma_r^2}, \quad (24)$$

$$\gamma_q = \kappa_q^2 + 2S\sigma_q^2, \quad (25)$$

$$\gamma_v = \sqrt{b^2 + a\sigma_v^2}, \quad (26)$$

²⁵ See his Appendix B, where transforms are based on Pan (2002)'s Appendix B and Duffie et al. (2000).

$$a = S(1 - S) - 2\lambda \left(\exp(S\mu_J + S^2 \frac{\sigma_J^2}{2}) - 1 - S\mu^* \right) - 2S\eta^S, \quad (27)$$

$$b = \sigma_v \rho S - \kappa_v. \quad (28)$$

Given the parameter estimates reported in Table 1 and the level of the underlying S , the physical density f_P can be obtained via numerical integration of

$$f_P(S; v, r, q, \tau) = \frac{1}{2\pi} \int_{-\infty}^{\infty} \psi(iz; v, r, q, \tau) \exp(-izS) dz. \quad (29)$$

To obtain the risk neutral density f_Q , some of the parameters have to be replaced by their risk neutral counterparts. The time- t conditional transform under the risk neutral measure is then given by

$$\psi^*(S; v, r, q, \tau) = \exp(\alpha_r(S) + \alpha_q(S) + \alpha_v^*(S) + \beta_r(S)r + \beta_q(S)q + \beta_v^*(S)v), \quad (30)$$

where α_r , α_q , β_r , and β_q are defined as in Eq. (17) and

$$\alpha_v^* = -\frac{\kappa_v^* \bar{v}^*}{\sigma_v^2} \left((\gamma_v^* + b^*)\tau + 2 \ln \left(1 - (\gamma_v^* + b^*) \frac{1 - \exp(-\gamma_v^* \tau)}{2\gamma_v^*} \right) \right), \quad (31)$$

$$\beta_v^* = -\frac{a^*(1 - \exp(-\gamma_v^* \tau))}{2\gamma_v^* - (\gamma_v^* + b^*)(1 - \exp(-\gamma_v^* \tau))}, \quad (32)$$

with

$$\kappa_v^* = \kappa_v - \eta^v, \quad (33)$$

$$\bar{v}^* = \kappa_v \bar{v} / \kappa_v^*, \quad (34)$$

$$a^* = S(1 - S) - 2\lambda (\exp(S\mu_J^* + S^2 \sigma_J^2 / 2) - 1 - S\mu^*), \quad (35)$$

$$b^* = \sigma_v \rho S - \kappa_v^*, \quad (36)$$

$$\gamma_v^* = \sqrt{(b^*)^2 + a^* \sigma_v^2}. \quad (37)$$

Given the parameter estimates reported in Table 1 and the level of the underlying S , f_Q can again be obtained via numerical integration:

$$f_Q(S; v, r, q, \tau) = \frac{1}{2\pi} \int_{-\infty}^{\infty} \psi^*(iz; v, r, q, \tau) \exp(-izS) dz. \quad (38)$$

Appendix B: alternative maturities—distributions

See Figs. 12 and 13.

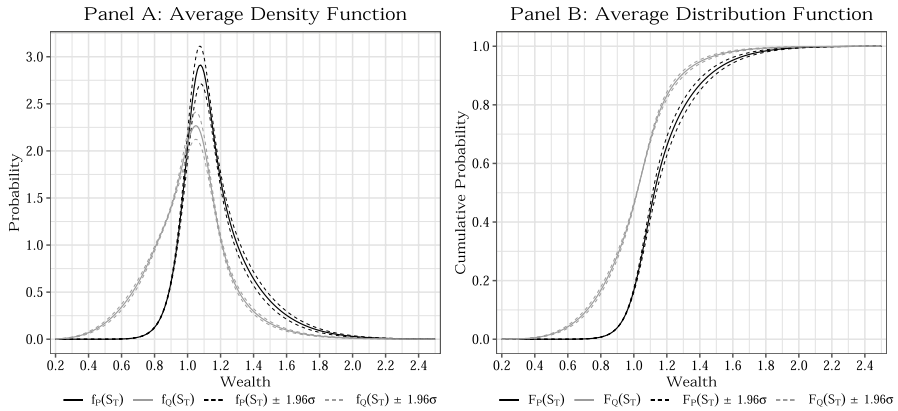


Fig. 12 Physical and Risk Neutral Distributions, 6 Months Horizon. This figure plots physical and risk neutral densities (Panel A) and distribution functions (Panel B), estimated from the Pan (2002) stochastic volatility and jumps model and averaged over volatilities from 0.01 to 0.60. Physical (risk neutral) densities are denoted by $f_p(S_T)$ ($f_Q(S_T)$), whereas physical (risk neutral) distribution functions are denoted by $F_p(S_T)$ ($F_Q(S_T)$). We assume a return horizon of 6 months

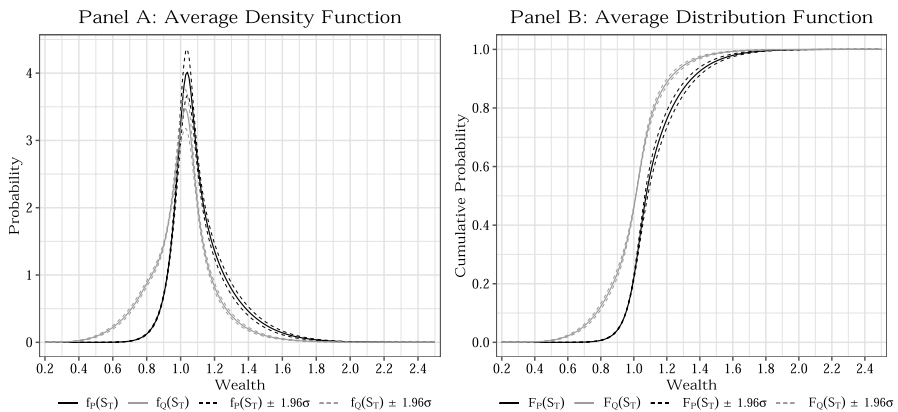


Fig. 13 Physical and Risk Neutral Distributions, 3 Months Horizon. This figure plots physical and risk neutral densities (Panel A) and distribution functions (Panel B), estimated from the Pan (2002) stochastic volatility and jumps model and averaged over volatilities from 0.01 to 0.60. Physical (risk neutral) densities are denoted by $f_p(S_T)$ ($f_Q(S_T)$), whereas physical (risk neutral) distribution functions are denoted by $F_p(S_T)$ ($F_Q(S_T)$). We assume a return horizon of 3 months

Appendix C: alternative maturities—pricing kernels

See Figs. 14 and 15.

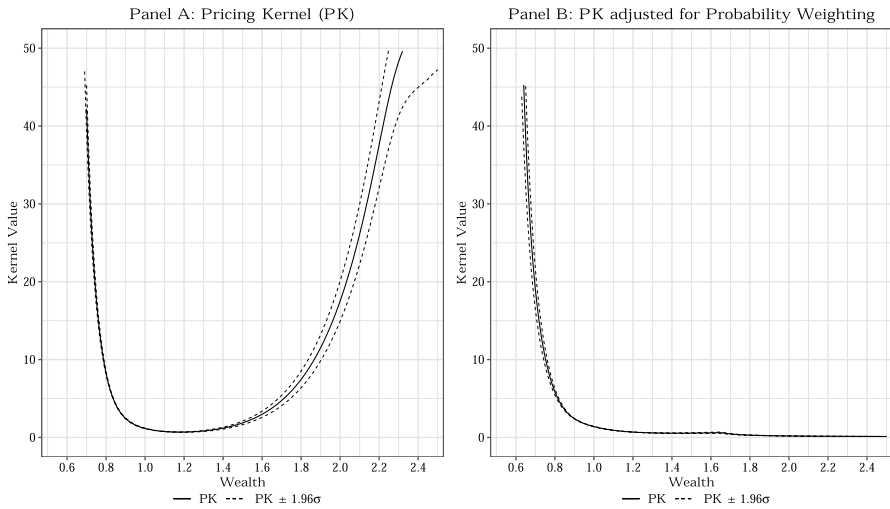


Fig. 14 Average Pricing Kernel, 6 Months Horizon. This figure plots pricing kernels estimated from the Pan (2002) stochastic volatility and jumps model. Following the literature (e.g. Jackwerth, 2000; Baele et al., 2019), we estimate the pricing kernel (PK, Panel A) as the ratio of the risk neutral to the physical probabilities, i.e $PK = f_Q/f_P$. In Panel B, we follow Eq. (1) and calculate the pricing kernel, net of probability weighting, as $PK = f_Q(S_T)/f_P(S_T) \cdot w'(1 - F_P(S_T))$. We assume a return horizon of 6 months

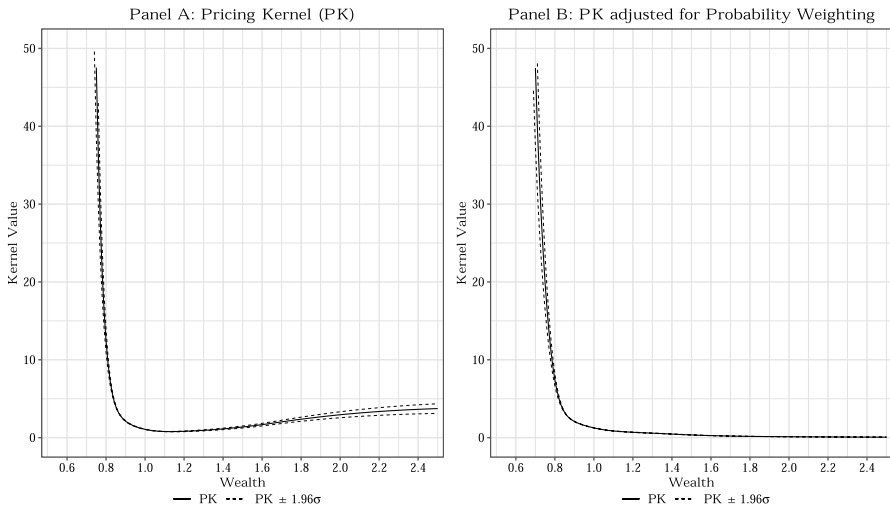


Fig. 15 Average Pricing Kernel, 3 Months Horizon. Figure 15 plots pricing kernels estimated from the Pan (2002) stochastic volatility and jumps model. Following the literature (e.g. Jackwerth, 2000; Baele et al., 2019), we estimate the pricing kernel (PK, Panel A) as the ratio of the risk neutral to the physical probabilities, i.e $PK = f_Q/f_P$. In Panel B, we follow Eq. (1) and calculate the pricing kernel, net of probability weighting, as $PK = f_Q(S_T)/f_P(S_T) \cdot w'(1 - F_P(S_T))$. We assume a return horizon of 3 months

Funding Open Access funding enabled and organized by Projekt DEAL.

Open Access This article is licensed under a Creative Commons Attribution 4.0 International License, which permits use, sharing, adaptation, distribution and reproduction in any medium or format, as long as you give appropriate credit to the original author(s) and the source, provide a link to the Creative Commons licence, and indicate if changes were made. The images or other third party material in this article are included in the article's Creative Commons licence, unless indicated otherwise in a credit line to the material. If material is not included in the article's Creative Commons licence and your intended use is not permitted by statutory regulation or exceeds the permitted use, you will need to obtain permission directly from the copyright holder. To view a copy of this licence, visit <http://creativecommons.org/licenses/by/4.0/>.

References

- Abdellaoui, M. (2000). Parameter-free elicitation of utility and probability weighting functions. *Management Science*, 46(11), 1497–1512. <https://doi.org/10.1287/mnsc.46.11.1497.12080>.
- Ait-Sahalia, Y., & Lo, A. W. (2000). Nonparametric risk management and implied risk aversion. *Journal of Econometrics*, 94(1), 9–51. [https://doi.org/10.1016/S0304-4076\(99\)00016-0](https://doi.org/10.1016/S0304-4076(99)00016-0)
- Babaoğlu, K., Christoffersen, P., Heston, S., & Jacobs, K. (2018). Option valuation with volatility components, fat tails, and nonmonotonic pricing kernels*. *The Review of Asset Pricing Studies*, 8(2), 183–231. <https://doi.org/10.1093/rapsu/rax021>
- Baele, L., Driessen, J., Ebert, S., Londono, J. M., & Spalt, O. G. (2019). Cumulative prospect theory, option returns, and the variance premium. *The Review of Financial Studies*, 32(9), 3667–3723. <https://doi.org/10.1093/rfs/hhy127>
- Baker, M., & Wurgler, J. (2000). The equity share in new issues and aggregate stock returns. *The Journal of Finance*, 55(5), 2219–2257. <https://doi.org/10.1111/0022-1082.00285>
- Bakshi, G., Madan, D., & Panayotov, G. (2010). Returns of claims on the upside and the viability of U-shaped pricing kernels. *Journal of Financial Economics*, 97(1), 130–154. <https://doi.org/10.1016/j.jfineco.2010.03.009>
- Barberis, N., Huang, M., & Santos, T. (2001). Prospect theory and asset prices*. *The Quarterly Journal of Economics*, 116(1), 1–53. <https://doi.org/10.1162/003355301556310>
- Barberis, N., Mukherjee, A., & Wang, B. (2016). Prospect theory and stock returns: An empirical test. *The Review of Financial Studies*, 29(11), 3068–3107. <https://doi.org/10.1093/rfs/hhw049>
- Bates, D. S. (2000). Post-'87 crash fears in the S&P 500 futures option market. *Journal of Econometrics*, 94(1), 181–238. [https://doi.org/10.1016/S0304-4076\(99\)00021-4](https://doi.org/10.1016/S0304-4076(99)00021-4)
- Beare, B. K., & Schmidt, L. D. W. (2016). An empirical test of pricing kernel monotonicity. *Journal of Applied Econometrics*, 31(2), 338–356. <https://doi.org/10.1002/jae.2422>
- Benzoni, L., Collin-Dufresne, P., & Goldstein, R. S. (2011). Explaining asset pricing puzzles associated with the 1987 market crash. *Journal of Financial Economics*, 101(3), 552–573. <https://doi.org/10.1016/j.jfineco.2011.01.008>
- Bleichrodt, H., & Pinto, J. L. (2000). A parameter-free elicitation of the probability weighting function in medical decision analysis. *Management Science*, 46(11), 1485–1496. <https://doi.org/10.1287/mnsc.46.11.1485.12086>
- Bliss, R. R., & Panigirtzoglou, N. (2004). Option-implied risk aversion estimates. *The Journal of Finance*, 59(1), 407–446. <https://doi.org/10.1111/j.1540-6261.2004.00637.x>
- Brandt, M. W., & Wang, K. Q. (2003). Time-varying risk aversion and unexpected inflation. *Journal of Monetary Economics*, 50(7), 1457–1498. <https://doi.org/10.1016/j.jmoneco.2003.08.001>
- Brown, D. P., & Jackwerth, J. C. (2012). The pricing kernel puzzle: Reconciling index option data and economic theory. In J. A. Batten & N. Wagner (Eds.), *Derivative securities pricing and modelling, volume 94 of contemporary studies in economic and financial analysis* (pp. 155–183). Emerald Group Publishing Limited. [https://doi.org/10.1108/S1569-3759\(2012\)0000094009](https://doi.org/10.1108/S1569-3759(2012)0000094009)
- Camerer, C. F., & Ho, T.-H. (1994). Violations of the betweenness axiom and nonlinearity in probability. *Journal of Risk and Uncertainty*, 8(2), 167–196. <https://doi.org/10.1007/BF01065371>

- Campbell, J., & Cochrane, J. (1999). By force of habit: A consumption-based explanation of aggregate stock market behavior. *Journal of Political Economy*, 107(2), 205–251. <https://doi.org/10.1086/250059>
- Chabi-Yo, F. (2012). Pricing kernels with stochastic skewness and volatility risk. *Management Science*, 58(3), 624–640. <https://doi.org/10.1287/mnsc.1110.1424>
- Chabi-Yo, F., Garcia, R., & Renault, E. (2008). State dependence can explain the risk aversion puzzle. *The Review of Financial Studies*, 21(2), 973–1011. <https://doi.org/10.1093/rfs/hhm070>
- Chen, Y.-W., Chou, R. K., & Lin, C.-B. (2019). Investor sentiment, SEO market timing, and stock price performance. *Journal of Empirical Finance*, 51, 28–43. <https://doi.org/10.1016/j.jempfin.2019.01.008>
- Christoffersen, P., Heston, S., & Jacobs, K. (2013). Capturing option anomalies with a variance-dependent pricing kernel. *The Review of Financial Studies*, 26(8), 1963–2006. <https://doi.org/10.1093/rfs/hht033>
- Cuesdeanu, H., & Jackwerth, J. C. (2018). The pricing kernel puzzle in forward looking data. *Review of Derivatives Research*, 21(3), 253–276. <https://doi.org/10.1007/s11147-017-9140-8>
- Dierkes, M. (2013). *Probability weighting and asset prices*. SSRN Scholarly Paper ID 2253817, Social Science Research Network, Rochester, NY. <https://doi.org/10.2139/ssrn.2253817>
- Dierkes, M., Krupski, J., & Schroen, S. (2022). Option-implied lottery demand and IPO returns. *Journal of Economic Dynamics and Control*. <https://doi.org/10.1016/j.jedc.2022.104356>
- Dierkes, M., & Sejdin, V. (2019). Indistinguishability of small probabilities, subproportionality, and the common ratio effect. *Journal of Mathematical Psychology*, 93, 102283. <https://doi.org/10.1016/j.jmp.2019.102283>
- Duffie, D., Pan, J., & Singleton, K. (2000). Transform analysis and asset pricing for affine jump-diffusions. *Econometrica*, 68(6), 1343–1376. <https://doi.org/10.1111/1468-0262.00164>
- Eraker, B., & Ready, M. (2015). Do investors overpay for stocks with lottery-like payoffs? An examination of the returns of OTC stocks. *Journal of Financial Economics*, 115(3), 486–504. <https://doi.org/10.1016/j.jfineco.2014.11.002>
- Fama, E. F. (2014). Two pillars of asset pricing. *American Economic Review*, 104(6), 1467–1485. <https://doi.org/10.1257/aer.104.6.1467>
- Gao, X., Koedijk, K. G., & Wang, Z. (2021). Volatility-dependent skewness preference. *The Journal of Portfolio Management*, 48(1), 43–58. <https://doi.org/10.3905/jpm.2021.1.295>
- Golubev, Y., Härdle, W. K., & Timofeev, R. (2014). Testing monotonicity of pricing kernels. *ASA Advances in Statistical Analysis*, 98(4), 305–326. <https://doi.org/10.1007/s10182-014-0225-5>
- Gonzalez, R., & Wu, G. (1999). On the shape of the probability weighting function. *Cognitive Psychology*, 38(1), 129–166. <https://doi.org/10.1006/cogp.1998.0710>
- Green, T. C., & Hwang, B.-H. (2012). Initial public offerings as lotteries: Skewness preference and first-day returns. *Management Science*, 58(2), 432–444. <https://doi.org/10.1287/mnsc.1110.1431>
- Guiso, L., Sapienza, P., & Zingales, L. (2018). Time varying risk aversion. *Journal of Financial Economics*, 128(3), 403–421. <https://doi.org/10.1016/j.jfineco.2018.02.007>
- Hens, T., & Reichlin, C. (2013). Three solutions to the pricing kernel puzzle. *Review of Finance*, 17(3), 1065–1098. <https://doi.org/10.1093/rof/rfs008>
- Jackwerth, J. C. (2000). Recovering risk aversion from option prices and realized returns. *The Review of Financial Studies*, 13(2), 433–451. <https://doi.org/10.1093/rfs/13.2.433>
- Jackwerth, J. C., & Rubinstein, M. (1996). Recovering probability distributions from option prices. *The Journal of Finance*, 51(5), 1611–1631. <https://doi.org/10.1111/j.1540-6261.1996.tb05219.x>
- Kilka, M., & Weber, M. (2001). What determines the shape of the probability weighting function under uncertainty? *Management Science*, 47(12), 1712–1726. <https://doi.org/10.1287/mnsc.47.12.1712.10239>
- Kliger, D., & Levy, O. (2009). Theories of choice under risk: Insights from financial markets. *Journal of Economic Behavior & Organization*, 71(2), 330–346. <https://doi.org/10.1016/j.jebo.2009.01.012>
- Linn, M., Shive, S., & Shumway, T. (2018). Pricing kernel monotonicity and conditional information. *The Review of Financial Studies*, 31(2), 493–531. <https://doi.org/10.1093/rfs/hhx095>
- Liu, J., Pan, J., & Wang, T. (2005). An equilibrium model of rare-event premia and its implication for option smirks. *The Review of Financial Studies*, 18(1), 131–164. <https://doi.org/10.1093/rfs/hhi011>

- Pan, J. (2002). The jump-risk premia implicit in options: Evidence from an integrated time-series study. *Journal of Financial Economics*, 63(1), 3–50. [https://doi.org/10.1016/S0304-405X\(01\)00088-5](https://doi.org/10.1016/S0304-405X(01)00088-5)
- Polkovnichenko, V., & Zhao, F. (2013). Probability weighting functions implied in options prices. *Journal of Financial Economics*, 107(3), 580–609. <https://doi.org/10.1016/j.jfineco.2012.09.008>
- Prelec, D. (1998). The probability weighting function. *Econometrica*, 66(3), 497–527. <https://doi.org/10.2307/2998573>
- Quiggin, J. (1993). *Generalized expected utility theory: The rank dependent model*. Springer.
- Rosenberg, J. V., & Engle, R. F. (2002). Empirical pricing kernels. *Journal of Financial Economics*, 64(3), 341–372. [https://doi.org/10.1016/S0304-405X\(02\)00128-9](https://doi.org/10.1016/S0304-405X(02)00128-9)
- Schneider, C., & Spalt, O. (2017). Acquisitions as lotteries? The selection of target-firm risk and its impact on merger outcomes. *Critical Finance Review*, 6(1), 77–132. <https://doi.org/10.1561/104.00000035>
- Song, Z., & Xiu, D. (2016). A tale of two option markets: Pricing kernels and volatility risk. *Journal of Econometrics*, 190(1), 176–196. <https://doi.org/10.1016/j.jeconom.2015.06.024>
- Stott, H. P. (2006). Cumulative prospect theory's functional menagerie. *Journal of Risk and Uncertainty*, 32(2), 101–130. <https://doi.org/10.1007/s11166-006-8289-6>
- Tversky, A., & Fox, C. R. (1995). Weighing risk and uncertainty. *Psychological Review*, 102(2), 269–283. <https://doi.org/10.1037/0033-295X.102.2.269>
- Tversky, A., & Kahneman, D. (1992). Advances in prospect theory: Cumulative representation of uncertainty. *Journal of Risk and Uncertainty*, 5(4), 297–323. <https://doi.org/10.1007/BF00122574>
- Wu, G., & Gonzalez, R. (1996). Curvature of the probability weighting function. *Management Science*, 42(12), 1676–1690. <https://doi.org/10.1287/mnsc.42.12.1676>
- Zeisberger, S., Vrecko, D., & Langer, T. (2012). Measuring the time stability of prospect theory preferences. *Theory and Decision*, 72(3), 359–386. <https://doi.org/10.1007/s11238-010-9234-3>
- Ziegler, A. (2007). Why does implied risk aversion smile? *The Review of Financial Studies*, 20(3), 859–904. <https://doi.org/10.1093/rfs/hhl023>

Publisher's Note Springer Nature remains neutral with regard to jurisdictional claims in published maps and institutional affiliations.

Authors and Affiliations

Maik Dierkes¹  · Jan Krupski¹ · Sebastian Schroen¹ · Philipp Sibbertsen²

✉ Maik Dierkes
maik.dierkes@finance.uni-hannover.de

Jan Krupski
jan.krupski@finance.uni-hannover.de

Sebastian Schroen
sebastian.schroen@finance.uni-hannover.de

Philipp Sibbertsen
sibbertsen@statistik.uni-hannover.de

¹ Institute of Banking and Finance, Leibniz University Hannover, Koenigsworther Platz 1, 30167 Hannover, Germany

² Institute of Statistics, Leibniz University Hannover, Koenigsworther Platz 1, 30167 Hannover, Germany